理學博士學位請求論文

Diet–Microbe interactions regulate biofilm formation and metabolic adaptation

박테리아에서 대사 신호에 따른

생물막 형성 및 대사 흐름 조절

2020년 8월

서울大學校 大學院

生命科學部

許 圭

Diet-Microbe interactions regulate biofilm formation and metabolic adaptation

by

Kyoo Heo

Under the supervision of

Professor Yeong-Jae Seok, Ph. D

A Thesis for the Degree of **Doctor of Philosophy**

August, 2020

School of Biological Sciences

Seoul National University

Abstract

Diet-Microbe interaction regulates biofilm formation and metabolic adaptation

Kyoo Heo

School of Biological Sciences

The Graduate School

Seoul National University

Bacteria exhibit an outstanding ability to respond to trivial fluctuations in their environments, developing various signal transduction systems sensing and responding to extracellular stimuli. Among them, bacteria possess sophisticated regulatory mechanisms to sense metabolic shifts, including nutrients, coordinating the overall biological processes in metabolism. In addition to its importance in the energy biogenesis and biomass synthesis, metabolic signals also provide environmental cues for bacteria living in various niches, a feature especially important for the pathogenic bacteria.

Here, I investigated two distinct regulatory mechanisms dependent on the metabolic signals. First, I present a novel role of phosphoenolpyruvate(PEP):carbohydrate phosphotransferase system (PTS) in the regulation of biofilm formation in pathogenic *Vibrio cholerae*. I found that glucose-specific Enzyme II ($EIIA^{Glc}$) of the PTS interacts with a c-di-GMP phosphodiesterase, mediating the regulation of the c-di-GMP level and

biofilm formation depending on the extracellular carbon sources. This system is expected to be a metabolic signal-dependent regulator which determine whether to stay or escape from its surrounding during host infection. I then suggest the mechanism how *Escherichia coli* responds to the shift in its metabolic flux. I revealed that malate dehydrogenase, one of the enzymes in tricarboxylic acid cycle, interacts with a lysine acetyltransferase PatZ and regulates the acetyltransferase activity of PatZ depending on the concentration of NADH. I found that PatZ decreases the gluconeogenesis/glycolysis flux ratio when *E. coli* grows on galactose or TCA intermedates, while this regulatory function of PatZ is inhibited by malate dehydrogenase in the presence of fermentative sugars, such as glucose, and fructose. Through these experiments, I propose a novel flux-dependent signal transduction system that mediates metabolic adaptation to various carbon sources.

Key words:

Metabolic signals, PEP:carbohydrate phosphotransferase system (PTS), c-di-GMP, flux-dependent signal transduction system, lysine acetyltransferase

***Student number*: 2014-21270**

Contents

List of Figures

List of Tables

Abbreviations

cAMP, cyclic AMP; 3' 5'-cyclic adenosine monophosphate

c-di-GMP, bis-(3'-5')-cyclic dimeric guanosine monophosphate

(p)ppGpp, guanosine 3'-diphosphate-5'-di(tri)phosphate

PTS, phosphoenolpyruvate: carbohydrate phosphotransferase system

EI, enzyme I of the PTS

HPr, histidine-containing phosphocarrier protein

$EIIA^{Glc}$, glucose specific-enzyme IIA subunit of PTS

Mdh, malate dehydrogenase

TCA, tricarboxylic acid cycle

Glc, glucose

NAG, N-acetylglucosamine

Mtl, mannitol

Fru, fructose

Succ, succinate

Mal, malate

Fum, fumarate

Gal, galactose

Pyr, pyruvate

AcCoA, acetyl coenzyme A

Chapter I. Literature Review

1. Phosphoenolpyruvate: carbohydrate phosphotransferase system (PTS) dependent signal transduction system

1.1 Overview of PTS-mediated regulation

Phosphoenolpyruvate (PEP):carbohydrate phosphotransferase system (PTS) is the most efficient sugar transport system in bacteria and is responsible for transporting more than 20 carbohydrates (Kundig et al., 1964; Postma et al., 1993). The PTS consists of two general components, enzyme I (EI) and histidine phosphocarrier protein (HPr) that participate in the transport of most PTS carbohydrates, and several sugar-specific components collectively known as enzyme IIs (EIIs). EI and HPr transfer a phosphoryl group from PEP to EII components, which finally phosphorylate PTS carbohydrates during their translocation across the membrane (Barabote and Saier, 2005; Postma et al., 1993; Tchieu et al., 2001).

It is knwon that the PTS regulates various cellular functions through its phosphorylation-dependent interactions with diverse proteins including transporter, transcription factors, second messenger-related molecules (Deutscher et al., 2014a). As the phosphorylation status of these PTS components reflects the availability of extracellular carbon sources and energy conditions, studies on PTS interactomes could reveal how bacteria respond to their nutritional status.

Previous studies have revealed that PTS components have different interacting-proteins among different species, suggesting that this signal transduction system has been evolved to have a species-specific role.

1.2 PTS-mediated regulations in *E. coli*

1.2.1 Carbon catabolite repression

Carbon catabolite repression (CCR) is a regulatory mechanism by which the expression or function of enzymes required for the utilization of secondary carbon sources is inhibited by the presence of a preferred source (Contesse et al., 1969; Loomis and Magasanik, 1967). This regulation allows bacteria to sequentially utilize the existing carbon sources, increasing the fitness by optimizing growth rates when they are exposed to more than one carbohydrate. In enteric bacteria, the CCR mechanism is generally dependent on the phosphorylation state of PTS components, especially glucose-specific enzyme IIA ($EIIA^{Glc}$) (Deutscher et al., 2006; Gorke and Stulke, 2008). When bacteria utilize glucose, which is the most preferred sugar in most bacteria, the components of the PTS are mostly dephosphorylated. The dephosphorylated $EIIA^{Glc}$ binds to non-PTS permeases, such as lactose permease LacY (Postma et al., 1993), and inhibits their transport activity, which is defined as "inducer exclusion". Simultaneously, the "induction prevention" is also observed in which the number of cAMP-CRP complex, the transcription activator of these permeases, decreases as only phosphorylated $EIIA^{Glc}$ can activate adenylate cyclase CyaA (Bettenbrock et al., 2007; Park et al., 2006). These two interactions by $EIIA^{Glc}$ enables bacteria to preferentially utilize glucose.

1.2.2 Rsd & SpoT

It has been reported that the dephosphorylated HPr interacts with and inhibits Rsd, which possesses the anti-sigma activity against the sigma factor RpoD (σ^{70}) (Park et al., 2013b). In cells growing exponentially by consuming PTS sugar, dephosphorylated HPr antagonizes the activity of Rsd so that σ^{70} can

bind to the core RNAP and express the σ^{70} housekeeping genes (Piper et al., 2009; Westblade et al., 2004). However, during the stationary phase when most nutrients are depleted, PTS components including HPr exist dominantly in the phosphorylated forms and HPr becomes incapable of sequestering Rsd. This enables σ^{S}, instead of σ^{70}, to bind to core RNAP and express stationary phage-related genes (Farewell et al., 1998; Gaal et al., 2001). In addition to its anti-sigma factor activity, Rsd has been reported to interact with a (p)ppGpp metabolizing enzyme SpoT (Lee et al., 2018). The interaction of Rsd with SpoT stimulates the (p)ppGpp hydrolase activity of SpoT and reduces the intracellular concentration of (p)ppGpp. Hence, the sequestration of Rsd by dephosphorylated HPr also acts on the regulation of the intracellular (p)ppGpp and controls regulatory mechanisms that coordinate resumption of growth during carbon source downshift (Hansen et al., 1975; Lazzarini et al., 1971).

1.3 PTS dependent regulation in *Vibrio* species

1.3.1 Motility

Bacterial chemotaxis and motility is a crucial factor for adaptation and propagation under nutrient fluctuations (Adler et al., 1973; Adler and Templeton, 1967; Dobrogosz and Hamilton, 1971). As the synthesis of flagellum requires a tremendous amount of cellular energy, the hierarchical expression of flagellar genes under strict control is conserved in most bacteria (Correa et al., 2005; Moisi et al., 2009). In *Vibrio vulnificus*, dephosphorylated glucose specific EIIA ($EIIA^{Glc}$) is known to interact with a flagella assembly protein (FapA) (Park et al., 2016; Park et al., 2019). Although the function of FapA is yet unknown, the recruitment of FapA to the pole by the polar landmark protein (HubP) is an essential factor for the formation of flagellum and bacterial motility. The interaction between $EIIA^{Glc}$

and FapA inhibits the polar localization of FapA, resulting in the detrimental effect on the flagellum formation. When glucose is sufficient, most $EIIA^{Glc}$ have dephosphorylated forms and sequester FapA from the cell pole, so that the cell stays in the glucose-sufficient environment and reduces unnecessary energy expenditure for the flagellum synthesis.

1.3.2 Biofilm formation

Biofilm is multicellular communities embedded in a self-produced polymeric matrix and play an important role in the persistence of bacterial infection (Flemming and Wingender, 2010; O'Toole et al., 2000). Also, dispersed cells from biofilm exhibit acute virulence and efficient transmission to other hosts, inferring that bacteria sophisticatedly regulate the biofilm formation under environmental fluctuations (Chua et al., 2014; Kaplan, 2010; Zhu and Mekalanos, 2003; Zhu et al., 2002). Recently, several studies have suggested the interaction between PTS system and biofilm formation in *Vibrio cholerae*. The deletion of PTS components, specifically EI, HPr, and $EIIA^{Glc}$ has affected the amount of biofilm formation (Houot et al., 2010a; Houot et al., 2010b). Also, global transcription regulator Mlc, functioning as a repressor of the expression of PTS, has been found to activate the *vps* gene which encodes Vibrio exopolysaccharide synthase, leading to biofilm formation (Pickering et al., 2014). Pull-down experiment with $EIIA^{Glc}$ resulted in the discovery of a novel interaction partner MshH, which represses biofilm formation (Pickering et al., 2012). Collectively, these findings suggest that PTS components are deeply involved in the regulation of biofilm formation but the operative mechanism has not been fully elucidated.

2. Flux-dependent signal transduction system

2.1 Overview of flux-dependent signal transduction system

The primary objective of living organisms is the uptake and metabolization of nutrients, generating ATP and synthesizing biomass. The metabolic fluxes are modulated by both intrinsic means, including gene expression, translation, and post-transcriptional regulation, and extracellular conditions, such as existing nutrients and air consumption. Thus, it is assumed that the metabolic fluxes represent the outcome of the orchestrated responses to the genuine metabolic status of the cell (Litsios et al., 2018). Recently, several studies have reported that bacteria could exhibit the phenotypic changes imposed by the shifts in metabolic fluxes, suggesting the presence of "flux-dependent signal transduction system" (Kochanowski et al., 2013; Kotte et al., 2010; Okano et al., 2020). In such system, the sensor enzyme detects the metabolic flux through the representative metabolites, called "flux-sensing metabolites", in which the information of the flux is stored in their concentrations. Sensor then transduces the flux information by the modulation of its enzymatic activity, or by transcriptional regulation and direct interaction with other proteins (Li et al., 2010; Link et al., 2013).

2.2 Example of flux-dependent signal transduction system

2.2.1 Overflow metabolism

When glucose uptake rate is low, cells can fully utilize the respiration for an efficient metabolism. However, in rapidly growing cells with high glucose uptake rate, the inefficient fermentation metabolism should be employed to prevent the accumulation of NADH, producing acetate, lactate, formate and succinate. This phenomenon, termed "overflow metabolism", can be

commonly observed among bacteria and yeast, or even in tumor cells and cancer cells where it is known as the Warburg effect (Warburg, 1956). In *E. coli*, it has been reported that the overflow metabolism is regulated by comparing the proteomic cost of energy biogenesis by respiration and that by fermentation. Quantitative proteome analysis suggested that when the energy biogenesis by the proteome-cost efficient fermentation is more efficient than that of respiration, this proteome cost information determines the level of overflow metabolism (Basan et al., 2015; Hui et al., 2015).

2.2.2 FBP

Fructose-1,6-bisphosphate (FBP) is one of the metabolic intermediates of the glycolysis pathway. In *E. coli*, the targeted metabolomics and mathematical simulation suggested that the glycolytic flux could be quantified and imprinted into the intracellular concentration of FBP, which correlates with the flux rate of glycolysis (Kochanowski et al., 2013). FBP interacts with a global transcription factor Cra, and represses the inhibitory effect of this transcription factor (Ramseier et al., 1995; Ramseier et al., 1993; Ryu et al., 1995; Shimada et al., 2011). As Cra is the transcription factor involved in the regulation of the expression of various enzymes in glycolysis and gluconeogenesis, it is expected that FBP-Cra interaction could be a strong flux sensor, regulating the metabolic enzymes depending on the upper glycolytic flux. Also, FBP is involved in the allosteric regulation of various enzymes including pyruvate kinase, phosphofructokinase and PEP carboxylase (Link et al., 2013; Zwaig and Lin, 1966), forming the feedforward activation of glycolysis. Collectively, FBP acts as a flux-sensing metabolite that stores the flux information of glycolysis.

2.2.3 cAMP-CRP

CRP (cAMP receptor protein) is the global regulator of genes for carbon source utilization in the absence of glucose. In *E. coli*, the synthesis of cAMP by adenylate cyclase is stimulated by the interaction with phosphorylated $EIIA^{Glc}$ of the PTS system (Park et al., 2006). Thus, cAMP-CRP system has been thought to be one of the canonical nutrient-sensors, which directly responds to extracellular cues. However, recent studies have suggested that the transcriptional activation by cAMP-CRP negatively correlates with growth rate under the variation of carbon nutrients and their uptake rates (Hermsen et al., 2015; Hui et al., 2015; You et al., 2013). Particularly, the expression of catabolic genes exhibits a gradual increase upon reduction in carbon influx or growth rate. Furthermore, the cAMP-CRP is involved in the allocation of proteomic resources under the overflow metabolism. These findings suggested that cAMP-CRP acts as a flux-sensing metabolites sensing the total influx of carbon sources and growth rates.

3. The aim of this study

The ability to sense and respond to changin environment is a crucial factor for the adaptation and proliferation of bacteria. It has been reported that PTS system is one of the sensory systems that senses environment-specific carbon sources and modulates various physiologies. Although PTS system is conserved among most bacteria, their structure and functions have species-specific variations. This study aims to assess a novel role of PTS system in the pathogenic *Vibrio cholerae* during host infection conditions.

Also, accumulating evidences suggested that bacterial cells could regulate their physiologies as a function of the actual intracellular metabolic fluxes, instead of direct sensing by nutrient-specific transmembrane or intracellular receptors. Here, I aim to find a novel flux-dependent signal transduction system and investigate its role in the regulation of metabolism in *E. coli*.

Chapter II. The sugar-mediated regulation of c-di-GMP phosphodiesterase in *Vibrio cholerae*

1. Abstract

Biofilm formation protects bacteria from stresses including antibiotics and host immune responses. Carbon sources can modulate biofilm formation and host colonization in *Vibrio cholerae*, but the underlying mechanisms remain unclear. Here, I show that $EIIA^{Glc}$, a component of the phosphoenolpyruvate (PEP):carbohydrate phosphotransferase system (PTS), regulates the intracellular concentration of the cyclic dinucleotide c-di-GMP and thus biofilm formation. The availability of preferred sugars such as glucose affects $EIIA^{Glc}$ phosphorylation state, which in turn modulates the interaction of $EIIA^{Glc}$ with a c-di-GMP phosphodiesterase (hereafter referred to as PdeS). In a *Drosophila* model of *V. cholerae* infection, sugars in the host diet regulate gut colonization in a manner dependent on the PdeS-$EIIA^{Glc}$ interaction. These results shed light into the mechanisms by which some nutrients regulate biofilm formation and host colonization.

2. Introduction

Most bacterial species can form biofilms, which are multicellular communities embedded in a self-produced polymeric matrix. The ability of pathogenic bacteria to form biofilms facilitates their colonization and persistence in the host due to the evasion of the immune response and increased resistance to many antimicrobials (Flemming and Wingender, 2010; O'Toole et al., 2000). In addition, it has been reported that dispersed cells exhibit acute virulence and efficient transmission to other hosts, indicating that an appropriate transition to planktonic cells from these sessile lifestyles is a crucial factor in their pathogenicity (Chua et al., 2014; Kaplan, 2010; Zhu and Mekalanos, 2003; Zhu et al., 2002). Thus, it is conceivable that sophisticated mechanisms should have evolved for pathogenic bacteria to regulate the transition between these two lifestyles in response to various environmental cues (Karatan and Watnick, 2009).

It has been shown that glucose and some other sugars in the environment induce the multilayer biofilm formation and the sugars promoting biofilm formation are substrates of the phosphoenolpyruvate (PEP):carbohydrate phosphotransferase system (PTS) in *V. cholerae* (Karatan and Watnick, 2009). This multi-component system mediates the transport of various sugars including glucose in *V. cholerae*, and these PTS sugars are concomitantly phosphorylated during transport (Hayes et al., 2017; Houot et al., 2010a). The PTS consists of two general components, enzyme I (EI) and histidine phosphocarrier protein (HPr) that participate in the transport of most PTS sugars, and several sugar-specific components collectively known as enzyme IIs (EIIs). EI and HPr transfer a phosphoryl group from PEP to EII components, which finally phosphorylate PTS carbohydrates during their translocation across the membrane.

In addition to its role in carbohydrate transport and phosphorylation, the PTS

acts as an efficient signal transduction system which can sense the availability of carbohydrates in the environment and thereby regulates various cellular functions (Deutscher et al., 2006). Phosphorylation of the PTS components usually increases in the absence and decreases in the presence of a PTS carbohydrate such as glucose (Hogema et al., 1998; Nam et al., 2005). Depending on their phosphorylation state, the PTS components regulate various sugar-related phenotypes by interacting with their cognate partners (Deutscher et al., 2014b). Although the effects of the PTS on biofilm formation have been reported in several studies (Houot et al., 2010a; Pickering et al., 2014; Pickering et al., 2012), the regulation mechanism of biofilm formation by the PTS has not been fully elucidated.

In enteric bacteria such as *Escherichia coli*, $EIIA^{Glc}$ (encoded by *crr*) is known to play multiple regulatory roles: dephosphorylated $EIIA^{Glc}$ inhibits non-PTS sugar permeases such as lactose permease and stimulates the fermentation/respiration switch protein FrsA (Deutscher et al., 2014b; Koo et al., 2004), whereas only phosphorylated $EIIA^{Glc}$ stimulates adenylate cyclase and thus increases the concentration of cAMP (Park et al., 2006), which is known to suppress biofilm formation in *V. cholerae* (Fong and Yildiz, 2008; Liang et al., 2007; Silva and Benitez, 2016). An interesting difference between the *E. coli* and *V. cholerae* PTS lies in the substrate specificity of $EIIA^{Glc}$. While $EIIA^{Glc}$ is specific for glucose in *E. coli*, its *V. cholerae* ortholog is shared among several PTS sugars such as *N*-acetylglucosamine, trehalose, and sucrose as well as glucose (Houot et al., 2010b). Therefore, it could be assumed that $EIIA^{Glc}$ may have distinct regulatory roles in response to several PTS sugars depending on the species. Unlike in E. coli, dephosphorylated $EIIA^{Glc}$ of *Vibrio vulnificus* inhibits flagella assembly and hence motility, allowing it to efficiently consume a preferable sugar in the environment (Park et al., 2016; Park et al., 2019). This regulation of the

transition from a motile to non-motile lifestyle mediated by $EIIA^{Glc}$ might also act on biofilm formation processes on the abiotic or biotic surfaces.

The regulatory functions of $EIIA^{Glc}$ on biofilm formation were suggested in *V. cholerae* in previous studies. $EIIA^{Glc}$ was shown to interact with MshH, a homolog of E. coli CsrD (Pickering et al., 2012), and a following study showed that dephosphorylated $EIIA^{Glc}$ activates CsrB/C turnover and increases the amount of CsrA (Leng et al., 2016), which is known to be a negative regulator of biofilm formation in several bacterial species (Jones et al., 2008; Vakulskas et al., 2015). It was also reported that cAMP, the reaction product of adenylate cyclase which is regulated by $EIIA^{Glc}$, and its receptor protein (CRP) directly and indirectly represses the expression of the diguanylate cyclase CdgA, which positively regulates biofilm formation in the *V. cholerae* C1552 strain (Beyhan et al., 2007; Fong and Yildiz, 2008). While the exogenous addition of cAMP represses the biofilm formation also in the *V. cholerae* MO10 strain, $EIIA^{Glc}$ was shown to activate biofilm formation in the presence of exogenous cAMP in this strain (Houot and Watnick, 2008). Collectively, these findings suggest the additional regulatory role of $EIIA^{Glc}$ on biofilm formation.

Here, I explored the molecular mechanism of how the biofilm formation is affected by carbon sources in *V. cholerae*. I find that $EIIA^{Glc}$ interacts with and modulates the activity of a c-di-GMP phosphodiesterase depending on its phosphorylation state and thereby regulates biofilm formation in the aquatic and host environment. I propose that $EIIA^{Glc}$ functions as a PTS sugar-responsive regulator of the c-di-GMP signaling pathway and determines whether to disperse from or stay in the biofilm in response to carbohydrates.

3. Materials and Methods

3.1. Bacterial strains, plasmids and culture conditions

The bacterial strains and plasmids used in this study are listed in Table II-1. Construction of the deletion strains was performed as described previously (Kim et al., 2015). *V. cholerae* strains were cultured in Luria-Bertani medium.

3.2. Purification of overexpressed proteins

While EI, HPr, and $EIIA^{Glc}$ were expressed in a *ptsHIcrr*-deleted ER2566 strain, other proteins were expressed in *E. coli* ER2566 by adding 1 mM IPTG. His-tagged proteins were purified using TALON metal-affinity resin (Takara Bio.) according to the manufacturer's instructions. After His-tagged proteins were eluted with 200 mM imidazole, the fractions containing His-tagged proteins were pooled and concentrated using Amicon Ultracel-3K centrifugal filters (Merck Millipore). To increase the purity of proteins and remove imidazole, the concentrated pool was chromatographed on a Hiload 16/60 Superdex 200 pg column (GE Healthcare) equilibrated with buffer A (25 mM HEPES-NaOH (pH 7.6), containing 100 mM NaCl, 10 mM β-mercaptoethanol, and 10% glycerol).

3.3. Ligand fishing using metal affinity beads

Ligand-fishing experiments were performed as described previously with minor modifications to find a new interaction partner of $EIIA^{Glc}$ (Park et al., 2019; Park et al., 2013a). *V. cholerae* O1 biovar El Tor N16961 cells grown at 37 ˚C overnight at LB (200 ml) were harvested and resuspended in buffer A. Cells were then disrupted by three passages through a French pressure cell at 8,000 psi. After centrifugation at 10,000 x g for 20 min at 4 ˚C, the

supernatant was mixed with 100 μg of His-EIIA^{Glc} or buffer A as control in the presence of TALON metal affinity resin in a 15-ml tube, then incubated at 4 ˚C for 30 min. His-EIIA^{Glc} was dephosphorylated by adding glucose or phosphorylated by adding PEP to the mixtures. After brief washes with buffer A containing 10 mM imidazole, the bound proteins were eluted with buffer A containing 200 mM imidazole and analyzed by SDS-PAGE using a 4-20% gradient Tris-glycine gel (KOMA biotech) and staining with Coomassie brilliant blue R. Protein bands specifically bound to the His-tagged bait protein were excised from the gel, and in-gel digestion and peptide mapping of the tryptic digests were performed using MALDI-TOF MS (Lee et al., 2018; Park et al., 2013a).

3.4. c-di-GMP phosphodiesterase activity assay using HPLC

c-di-GMP phosphodiesterase (PDE) activity was determined by measuring the remaining c-di-GMP and produced pGpG after the reaction (Schmidt et al., 2005). The reaction contained 20 mM Tris-HCl (pH 8.0), 50 mM NaCl, 5 mM $MgCl_2$, 0.5 mM EDTA, and 20 μM c-di-GMP in addition to PdeS in a total volume of 40 μl. To test the effect of the phosphorylation state of EIIA^{Glc} on PDE activity, EIIA^{Glc} and 0.4 μM of EI and HPr were added in the presence or absence of PEP. The phosphorylation states of EIIA^{Glc} were confirmed by SDS-PAGE and staining with Coomassie brilliant blue R (Hogema et al., 1998). The enzymatic reaction was started by the addition of c-di-GMP and allowed to proceed at 37 ˚C. Aliquots of each reaction were taken at appropriate times and reactions were stopped by adding 10 mM $CaCl_2$. These mixtures were boiled for 5 min and centrifuged. Then 20 μl of each supernatant was injected into a Supelcosil LC-18-T column (Sigma-Aldrich) using an Agilent HP1200 HPLC system (Agilent Technology). The

separations of pGpG and c-di-GMP were performed by gradient elution at a flow rate of 1.0 ml min^{-1} and chromatograms were recorded at 254 nm. The gradient program was: 0-5 min, isocratic elution with 100 mM potassium phosphate, pH 6.0 (A); 5-13 min, linear gradient to 70% A and 30% methanol (B); 13-16 min, isocratic at B; 16-18 min, linear gradient to A; 18-20 min, isocratic at A.

3.5. Determination of the intracellular concentration of c-di-GMP

V. cholerae was cultivated in LB medium (100 ml) to OD_{600} ~1.0, and centrifuged at 4,000 x g for 10 min. The cell pellet was resuspended in 500 µl extraction buffer (40% methanol, 40% acetonitrile, and 0.1 N formic acid) and incubated on ice for 15 min. Each sample was subjected to three cycles of freezing/thawing using liquid nitrogen and heat block adjusted to 90 ˚C. After an additional 15-min incubation on ice, the sample was centrifuged at 16,100 x g for 10 min, and 400 µl of the supernatant was dried under vacuum. The lyophilized nucleotides were resuspended in 80 µl of distilled water.

Quantification of the c-di-GMP was carried out using HPLC coupled with triple quadrupole mass spectrometry. The temperatures of the column oven and autosampler were maintained at 25 ˚C and 20 ˚C, respectively. Ten microliters of the resuspended nucleotides were injected to a Hypersil GOLD C column (2.1 x 100 mm, particle size 1.9 µM, pore size 175 Å, Thermo Scientific) using Accela 1250 UPLCTM system (Thermo Fisher Scientific, USA). Separation of c-di-GMP was performed using the following gradient program: solvent A, 20 mM ammonium acetate adjusted to pH 8.0 with ammonium hydroxide; solvent B, acetonitrile (ACN); flow rate 250 µl min-1; gradient condition, 0-2 min (15% B), 2-29 min (15-98% B), 29-33 min (98% B), 33-35 min (98-15% B), 35-45 min (15% B). Xanthosine 3',5'-cyclic

monophosphate (cXMP; BioLog) was used as an internal standard. The retention times for c-di-GMP and cXMP were 21.5 min and 16.8 min, respectively. The analyte detection was performed using TSQ Quantum Access Max (Thermo Scientific). Tune parameters for TSQ were as follows: capillary temperature, 300 ˚C; vaporization temperature, 250 ˚C; sheath gas pressure, 30 psi; aux gas pressure, 10 psi; positive polarity spray voltage, 4.0 kV. The samples were monitored with SRM scan mode. The SRM settings for c-di-GMP and cXMP were optimized and determined as follows: c-di-GMP: $[M + H]^+$ m/z 691 → 152; collision energy, 38 eV; cXMP: $[M + H]^+$ m/z 347 → 153, collision energy, 18 eV. The measured intracellular concentration of c-di-GMP was normalized with the protein level.

3.6. Microscale thermophoresis (MST) analysis

The binding affinities of PdeS with $EIIA^{Glc}$ and c-di-GMP were measured using a NanoTemper Monolith NT.115pico instrument (Bang et al., 2018). Purified GST-PdeS was labeled with NT-647 using a Monolith protein labeling kit and used at a concentration of 4.875 nM. Each unlabeled $EIIA^{Glc}$ and c-di-GMP was titrated in 1:1 serial dilutions in MST binding buffer (25 mM HEPES-NaOH (pH 7.6), 100 mM NaCl, 5 mM β-mercaptoethanol, 0.5 mg ml^{-1} BSA, 0.05 (v/v) % Tween 20), with the highest concentration of $EIIA^{Glc}$ at 21.9 μM and c-di-GMP at 500 μM. To prevent degradation of c-di-GMP by PdeS during the assay, their interaction was examined in the buffer without divalent cations which are indispensable for the PDE activity of PdeS. The measurements were performed at 15% LED power and 30% MST power at 22 ˚C.

3.7. Measurement of biofilm formation

Overnight-grown cells were inoculated in LB medium buffered with 40 mM potassium phosphate (pH 7.0) in the absence or presence of sugar and incubated under static conditions in a borosilicate tube at 37 ˚C for 23 h. After planktonic cells were washed away with PBS, the remaining biofilm-associated cells were stained with 0.1% crystal violet (CV) for 20 min. After rinses with PBS three times, the CV-stained biofilm was solubilized with 95% ethanol and measured at 550 nm (Lee et al., 2013; Watnick and Kolter, 1999). Mature biofilm was also visualized as described previously64 using confocal laser scanning microscopy (LSM700, Zeiss). *V. cholerae* strains constitutively expressing green fluorescent protein (GFP) were used for biofilm imaging.

3.8. Determination of the phosphorylation state of $EIIA^{Glc}$

The phosphorylation state of $EIIA^{Glc}$ was determined as described previously (Hogema et al., 1998; Lee et al., 2019) with some modifications. A 0.2-ml aliquot of cell culture was quenched at OD_{600} ~ 0.5 by adding 20 μl of 5 M NaOH followed by vortexing for 15 s, and then 150 μl of 3 M sodium acetate (pH 5.3) and 0.9 ml of ethanol were sequentially added. After incubated at -80 ˚C for 30 min, each sample was centrifuged at 10,000 x g at 4 ˚C for 30 min, and the pellet was resuspended in 40 μl of SDS sample buffer. A 20-μl aliquot of each sample was then resolved by SDS-PAGE using a 4-20% gradient gel, and $EIIA^{Glc}$ was visualized by western blot using anti-$EIIA^{Glc}$ serum (Nam et al., 2005).

3.9. Measurement of the cellular protein level by western blot

A *V. cholerae* strain in which the chromosomal vc1710 was tagged with 3xFLAG at its C-terminus was grown in LB medium and aliquots were harvested when OD_{600} reached 0.4, 1.0, and 1.5, respectively. After the pellets were resuspended in SDS loading buffer, cells were lysed by boiling for 5 min. Cell lysates were electrophoresed on a SDS-PAGE gel with various amounts of purified VC1710::3xFLAG protein or $EIIA^{Glc}$ as control. For immunodetection, monoclonal mouse anti-FLAG antibody (Sigma-Aldrich) or anti-$EIIA^{Glc}$ mouse serum was used.

3.10. Quantification of *V. cholerae* colonization in the fly intestine

To establish whether sugars could affect the gut colonization of *V. cholerae* strains, fasted adult flies (*Drosophila melanogaster w1118*) were orally administered a 5% sugar solution containing ~106 cells μl^{-1} of the *V. cholerae* strains in the presence of either glucose or mannitol for 24 h, and fed the same, but sterile, medium for another 9 h. After each fly was immersed in 70% ethanol for 3 min, the surface-sterilized fly was homogenized in 1 ml of sterile PBS and spread on LB agar plates containing 10 $\mu g\ ml^{-1}$ of streptomycin to determine colony-forming units of *V. cholerae*. To image bacterial infection, the whole alimentary canal was dissected at the same time point, and visualized by confocal laser scanning microscopy.

For measurement of food consumption, the feeding assay was performed with a standard method using FD&C Blue #1 dye (Ha et al., 2009). Flies were orally administered a 5% sugar (glucose or mannitol) solution containing *V. cholerae* cells and 0.5% (w/v) FD&C #1 dye for 2 h. Guts dissected from five flies were homogenized in 200 μl of PBS and the homogenate were centrifuged at 8,000 x g for 10 min. Food consumption was quantified by

measuring absorbance of the supernatant at 625 nm.

Table II-1. Bacterial strains and plasmids used in this study

Strain or Plasmid	Genotype or phenotype	Source
Strains		
Vibrio cholerae		
N16961	Wildtype, Clinical isolate	
N16961 Δ*pdeS*	N16961 with Δ*vc1710*	This study
N16961 Δ*crr*	N16961 with Δ*crr*	This study
N16961 *crr*(H91A)	N16961 in which the chromosomal $EIIA^{Glc}$ was substituted with dephosphomimetic form (H91A) of $EIIA^{Glc}$	This study
N16961 Δ*pdeS* *crr*(H91A)	N16961 with Δ*vc1710* in which the chromosomal $EIIA^{Glc}$ was substituted with dephosphomimetic form (H91A) of $EIIA^{Glc}$	This study
N16961 *vc1710::3x FLAG*	N16961 in which the chromosomal VC1710 was tagged with 3x FLAG at its c-terminus	This study
N16961 Δ*vpsA*	N16961 with Δ*vpsA*	This study
N16961 Δ*vpsA pdeS*	N16961 with Δ*vpsA pdeS*	This study
Escherichia coli		
ER2566	F^- I^- *fhuA2* [lon] *ompT lacZ*::*T7* gene 1 *gal sulA11* Δ(*mcrC*-mrr)114::IS10 R(*mcr*-73::miniTn10-TetS)2 R(*zgb*-210::Tn10)(TetS) *endA1* [*dcm*]	New England Biolabs

SM10 λ*pir*	*thi-1 thr leu tonA lacY supE recA*::RP4-2-Tc::Mu λ*pir*, OriT of RP4, Km^r; conjugational donor	(Miller *et al*.,1988)
Plasmids		
pDM4	Suicide vector for homologous recombination into *V. cholerae* chromosome, OriR6K, Cm^r	(Milton *et al*., 1996)
pETDuet-1		Novagen
pJK1113	pBAD24 with *oriT* of RP4 and *nptI*, P_{BAD}; Km^r , Amp^r	(Lim *et al*., 2014)
pBAD-MycHisA		Invitrogen
pDM4-*vc1710*	pDM4-based suicide vector for deletion of *vc1710*, Cm^r	This Study
pDM4-*crr*	pDM4-based suicide vector for deletion of *crr*, Cm^r	This Study
pET-HisCrr	pETDuet-1-based expression vector for His-$EIIA^{Glc}$, Amp^r	This Study
pET-Crr	pETDuet-1-based expression vector for $EIIA^{Glc}$, Amp^r	This Study
pET-VC1710	pETDuet-1-based expression vector for VC1710, Amp^r	This Study
pET-VC1710::3x FLAG	pETDuet-1-based expression vector for 3x FLAG tagged VC1710, Amp^r	This Study
pET-VCA1085	pETDuet-1-based expression vector for VCA1085 (VcFapA), Amp^r	This Study
pBAD-VC1710	pBAD-MycHisA-based expression vector for VC1710, Amp^r	This Study
pBAD-VC1710(E450A)	pBAD-MycHisA-based expression vector for VC1710(E450A), Amp^r	This Study

pJK1113-Crr	pJK1113-based expression vector for $EIIA^{Glc,}$ Amp^r, Km^r	This Study
pJK1113-Crr(H91A)	pJK1113-based expression vector for $EIIA^{Glc}$(H91A), Amp^r, Km^r	This Study
pKT25-Crr(H91A)	pKT25-based expression vector for $EIIA^{Glc}$(H91A), Km^r	This Study
pJK1113-P_{lac}::GFP	pJK1113-based expression vector for GFP driven by the *lac* promoter, Amp^r, Km^r	This Study

4. Results

4.1. EIIA^{Glc} interacts with an EAL domain-containing protein in *V. cholerae*.

In many bacteria, EIIA^{Glc} has been implicated in various sugar-dependent regulatory functions (Deutscher et al., 2014b). While it was suggested that EIIA^{Glc} participates in the regulation of biofilm formation in the presence of PTS carbohydrates in *V. cholerae* (Houot et al., 2010a; Pickering et al., 2014), no operative mechanisms were yet offered. To examine the effects of EIIA^{Glc} on biofilm formation, I measured biofilm production in the presence and absence of glucose. While wild-type *V. cholerae* had a higher level of biofilm formation in the presence of glucose than its absence, which was consistent with previous reports (Kierek and Watnick, 2003; Singh et al., 2017), a *crr*-deficient mutant exhibited no difference between the two conditions (Figure II-1a). Interestingly, while the *crr* mutant had a similar growth (Figure II-1b), this mutant exhibited a higher level of biofilm formation compared to the wild-type strain in LB medium (Figure II-1a), which is contrary to a previous study (Houot et al., 2010a). The exogenous addition of cAMP did not significantly alter the sugar effect, indicating that the regulation of biofilm formation by EIIA^{Glc} is independent of cAMP. These results led us to search for the regulator of biofilm formation, which transduces the sugar signal by directly interacting with EIIA^{Glc} in *V. cholerae*.

To find a new interaction partner of EIIA^{Glc}, I performed ligand fishing experiments using hexahistidine-tagged EIIA^{Glc} (His-EIIA^{Glc}) as bait (Park et al., 2016). Total proteins extracted from wild-type *V. cholerae* O1 biovar El Tor N16961 cells grown overnight at 37 ˚C were mixed with TALON metal affinity resin in the absence and presence of purified His-EIIA^{Glc}. His-EIIA^{Glc} was dephosphorylated by adding glucose or phosphorylated by adding PEP to the mixtures. After several washes, total proteins bound to the resins were

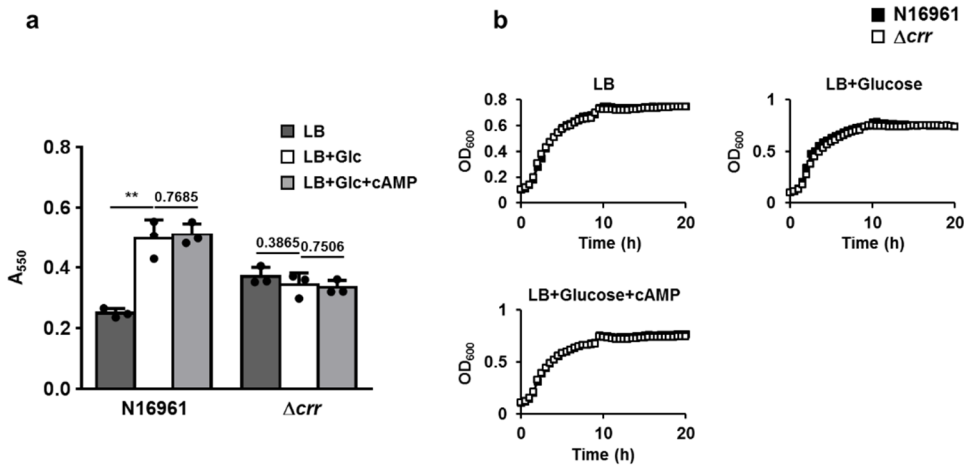

Figure II-1. EIIA^{Glc} enhances the biofilm formation in the presence of glucose in *Vibrio cholerae.*

a, The biofilm-forming activity of wild-type *V. cholerae* N16961 and an otherwise isogenic Δ*crr* mutant was measured in LB alone or supplemented with glucose or glucose and cAMP, as indicated. Biofilm formation was assessed following the static growth of *V. cholerae* cells for 23 h using a crystal violet staining method. The stained biofilm formation was determined 550 nm. Statistical significance was assessed using Student's *t*-test (*p values* greater than 0.05 were presented, ***p* value <0.01). Shown are the means and SD (n=3, independent measurements). **b,** Growth curves of the Δ*crr* mutant was compared with the wild-type *V. cholerae* N16961 strain in buffered LB medium supplemented with the indicated compounds (carbon sources to 0.1%, cAMP to 5 mM).

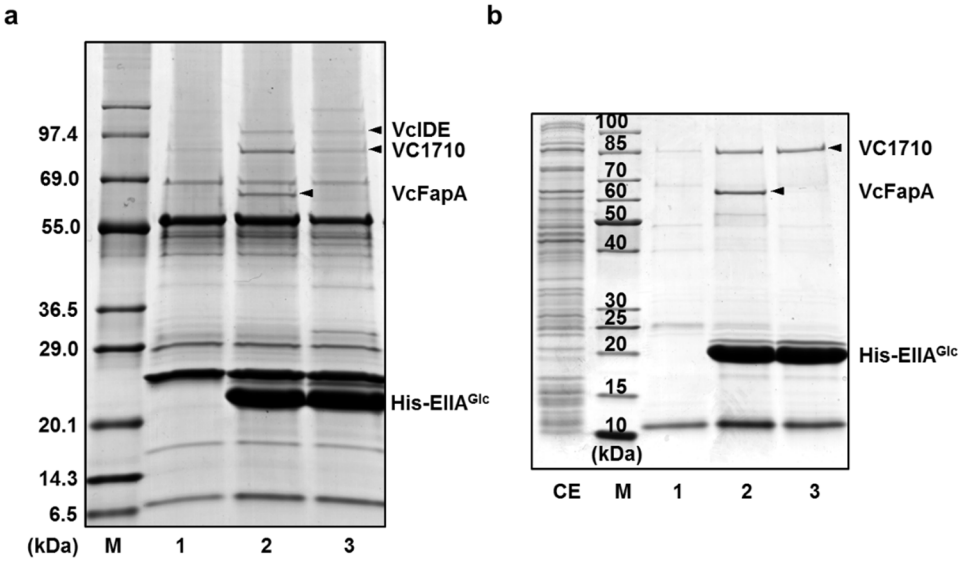

Figure II-2. EIIA^{Glc} interacts with a novel c-di-GMP phosphodiesterase VC1710.

a, Ligand fishing experiment was carried out to find proteins interacting with His-EIIA^{Glc}. Crude extract prepared from *V. cholerae* O1 biovar El Tor N16961 cells was mixed with buffer A (lane 1) or 100 μg of purified His-EIIA^{Glc} (lanes 2 and 3). The extract containing His-EIIA^{Glc} was supplemented with either 2 mM glucose to dephosphorylate EIIA^{Glc} (lane 2) or 2 mM PEP to phosphorylate EIIA^{Glc} (lane 3). Each mixture was subjected to TALON metal affinity chromatography and proteins bound to the column were analyzed as described in Materials and Methods. **b,** A mixture of *E. coli* cell lysates expressing recombinant VC1710 and VCA1085 (*V. cholerae* FapA) (lane CE) was mixed with buffer A or His-EIIA^{Glc} and subjected to TALON metal affinity chromatography as in panel a.

eluted with 200 mM imidazole and analyzed by SDS-PAGE and staining with Coomassie brilliant blue R (Figure II-2a). In repeated experiments, I could find three protein bands migrating with apparent molecular masses of approximately 100, 90 and 60 kDa, respectively, that were significantly and reproducibly enriched in the fraction containing both His-EIIA^{Glc} and glucose (lane 2). Peptide mapping of these proteins following in-gel tryptic digestion revealed that the protein band migrating at ~100 kDa corresponded to VC2072, an ortholog of the insulin-degrading enzyme IDE (VcIDE) (Kim et al., 2010), and the band at ~60 kDa to VCA1085, an ortholog of the flagella assembly protein FapA (VcFapA) (Park et al., 2016). Since IDE and FapA were already reported to interact with EIIA^{Glc} in *V. vulnificus* (Kim et al., 2010; Park et al., 2016), the elution of the two proteins only in the fraction containing His-EIIA^{Glc} indicates the reliability of this ligand fishing method (compare lanes 1 and 2). Interestingly, the band at ~90 kDa was identified as a putative EAL domain-containing c-di-GMP phosphodiesterase encoded by vc1710. The EAL domain is responsible for degrading bis-(3'-5')-cyclic diguanosine monophosphate (c-di-GMP) to pGpG (Galperin et al., 2001), which is known to repress biofilm formation and induce biofilm dispersion. Thus, I assumed that the interaction of EIIA^{Glc} with this EAL domain protein might be implicated in biofilm formation as a response to the sugar signal.

Interactions of a PTS component with its target proteins are usually dependent on the phosphorylation state of that PTS component. While the specific interaction between IDE and EIIA^{Glc} was reported to be independent of the phosphorylation state of EIIA^{Glc} (Kim et al., 2010), FapA was shown to interact only with dephosphorylated EIIA^{Glc} in *Vibrio vulnificus* (Park et al., 2016). In accordance with these previous studies, VcFapA was not co-eluted with His-EIIA^{Glc} in the fraction incubated with PEP (lane 3 in Figure II-2a), while the VcIDE band was clearly detected in the eluted fraction containing

phosphorylated His-EIIA^{Glc}. Since VC1710 band was detected in the two fractions incubated with EIIA^{Glc} and either glucose or PEP, I assumed that VC1710 interacts with both dephosphorylated and phosphorylated EIIA^{Glc}. To validate the ligand-fishing data, His-EIIA^{Glc}, EI, and HPr was mixed with glucose or PEP, and the phosphorylation state of His-EIIA^{Glc} was confirmed by its mobility shift in an SDS-PAGE gel first (Lee et al., 2019). Then a mixture of *E. coli* cell extracts expressing recombinant VC1710 and VcFapA (lane CE) was added and subjected to protein affinity pull-down assays to determine their interaction with either form of EIIA^{Glc} (lanes 2 and 3 in Figure II2-b). As expected, while VcFapA interacted only with dephosphorylated EIIA^{Glc}, VC1710 appeared to interact with both the dephosphorylated and phosphorylated forms of EIIA^{Glc}.

For quantitative analysis of the binding affinity of VC1710 for EIIA^{Glc}, the dissociation constants (K_d) of VC1710 complexed with dephosphorylated and phosphorylated EIIA^{Glc} (P~EIIA^{Glc}) were measured by microscale thermophoresis (MST) experiments. VC1710 showed a slightly higher affinity toward the dephosphorylated form of EIIA^{Glc} (Kd=114.1 ± 13.7 nM) than toward phosphorylated EIIA^{Glc} (286.7 ± 39.5 nM) (Figure II-3). This tight interaction of VC1710 with EIIA^{Glc} led us to assume that the physiological form of VC1710 exists as a complex with EIIA^{Glc} and the activity of VC1710 can be influenced by the phosphorylation state of EIIA^{Glc}, as exemplified by the interaction of adenylate cyclase with EIIA^{Glc} in *E. coli* (Park et al., 2006).

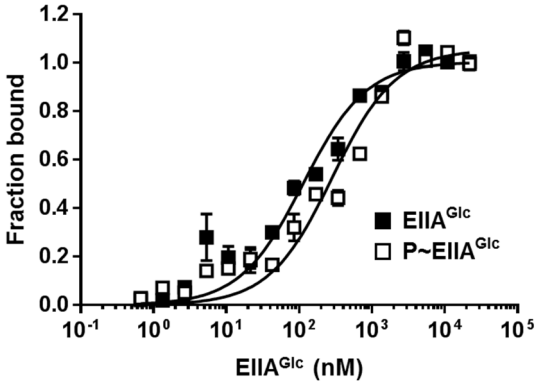

Figure II-3. EIIA^{Glc} interacts with VC1710 in the manner dependent on its phosphorylation state.

The binding affinities of VC1710 with either dephosphorylated (black square) or phosphorylated EIIA^{Glc} (white square) were measured using NanoTemper Monolith NT.115pico. The dissociation constants (K_d) of VC1710 complexed with dephosphorylated and phosphorylated EIIA^{Glc} (P~EIIA^{Glc}) were obtained from three technical replicates. Shown are the means and SD (n=3, independent measurements).

4.2 $EIIA^{Glc}$ regulates c-di-GMP phosphodiesterase activity of VC1710.

An analysis of the primary structure of VC1710 indicated that this protein consists of a PAS sensing domain in the N-terminus and an EAL domain predicted to encode a c-di-GMP phosphodiesterase (PDE) in the C-terminus (Tchigvintsev et al., 2010). It has also been previously reported that VC1710 binds c-di-GMP (Roelofs et al., 2015), suggesting its function in c-di-GMP metabolism. To determine whether VC1710 possesses PDE activity, I purified VC1710 and performed an in vitro PDE activity assay by reverse-phase HPLC. The concentration of remaining c-di-GMP decreased with a concomitant increase in the product pGpG after incubation with VC1710, and I could therefore confirm that VC1710 exhibited the predicted c-di-GMP hydrolytic activity (Figure II-4a, b). Then, to investigate if the PDE activity of VC1710 was affected by its interaction with $EIIA^{Glc}$, dephosphorylated or phosphorylated $EIIA^{Glc}$ was added to the reaction mixture. The phosphorylation states of $EIIA^{Glc}$ could be successfully modulated by incubation with EI, HPr and PEP, as shown in the SDS-PAGE analysis (Figure II-4c). When phosphorylated $EIIA^{Glc}$ was mixed with VC1710, the PDE activity was higher than that in the absence of $EIIA^{Glc}$. However, no c-di-GMP was digested in the reaction incubated with dephosphorylated $EIIA^{Glc}$, suggesting that dephosphorylated $EIIA^{Glc}$ inactivates the PDE activity of VC1710. To elucidate the kinetic properties of the VC1710 protein, I determined K_m and V_{max} values based on three independent activity assays. When c-di-GMP was reacted with VC1710 alone, the Km value was ~4.58 μM. However, when phosphorylated $EIIA^{Glc}$ was added to the VC1710 reaction mixture, the K_m value for c-di-GMP decreased to 1.30 μM (Figure II-5). Given that the K_d values for c-di-GMP-binding proteins ranged up to several μM and the K_m values of PDEs ranged from 60 nM to several μM (Hengge, 2009), the K_m values of VC1710 for c-di-GMP appear to be

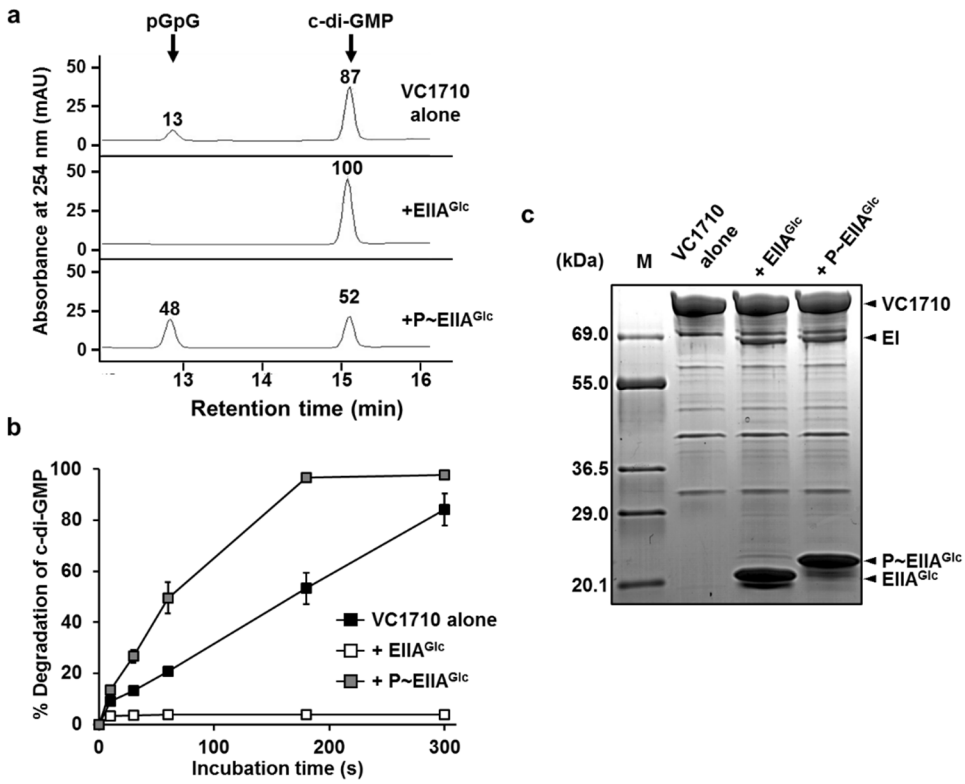

Figure II-4. EIIA^{Glc} modulates the PDE activity of VC1710 in a phosphorylation state-dependent manner.

a, The c-di-GMP phosphodiesterase (PDE) activity of VC1710 (4.1 μM) was assayed in a reaction mixture containing 20 μM of c-di-GMP and 0.4 μM of EI and HPr in the absence or presence of purified EIIA^{Glc} (17.1 μM). EIIA^{Glc} in the reaction mixture was phosphorylated by adding 2 mM PEP. The reaction mixtures were applied to a Supercosil LC-18-T HPLC column, and the remaining c-di-GMP and produced pGpG were quantified by measuring absorbance at 254 nm. **b,** The c-di-GMP hydrolysis activity of VC1710 was assessed in the absence (black square) and presence of EIIA^{Glc} (white and gray squares) as in panel **a**, and c-di-GMP and pGpG were analyzed at 0, 10, 30,

60, 180, and 300 s. **c**, The phosphorylation state of $EIIA^{Glc}$ in panels **a** and **b** was confirmed by SDS-PAGE and staining with Coomassie brilliant blue R

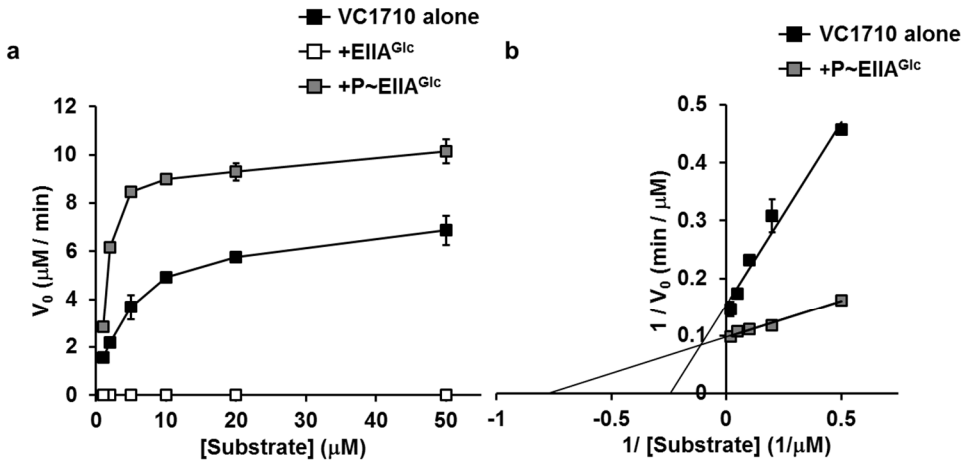

	K_m (μM)	V_{max} (μM min^{-1})
VC1710 alone	4.58±0.12	6.88±0.60
+ P~EIIA^{Glc}	1.30±0.08	10.15±0.51

Figure II-5 The kinetic properties of c-di-GMP hydrolysis by VC1710.

The Michaelis-Menten constant (K_m) and the maximum initial velocity (V_{max}) were determined for the VC1710-catalyzed hydrolysis of c-di-GMP. **a,** The initial velocity (V_0) of c-di-GMP hydrolysis was determined as described in Methods with 4.1 μM of VC1710 and was plotted as a function of c-di-GMP concentration (black square). The effect of EIIA^{Glc} on the enzyme kinetics of VC1710 was examined by adding approximately a 4 times molar excess of dephosphorylated (white square) or phosphorylated (gray square) EIIA^{Glc} to the reaction mixture. EIIA^{Glc} was phosphorylated by adding 2 mM PEP and 0.4 μM of EI and HPr. **b,** Lineweaver-Burk plots of the data in panel **a**.

biochemically and physiologically relevant to the control of the c-di-GMP level and thereby related phenotypes in vivo. To exclude the possibility of carrier protein effect, I performed the same experiment without $EIIA^{Glc}$ or in the presence of the same amount of BSA, and no measurable effect was detected (Figure II-6). The analytical western blot data (Figure II-7) shows that the number of the $EIIA^{Glc}$ protein in a *V. cholerae* cell is more than 100 times higher than that of the VC1710 protein. I, therefore, conclude that VC1710 is always present in a complex form with $EIIA^{Glc}$ in the cell and that the activity of VC1710 is entirely dependent on the phosphorylation state of $EIIA^{Glc}$. As the phosphorylation state of $EIIA^{Glc}$ was altered in response to the type of sugars (Nam et al., 2005), I named VC1710 as PdeS (for **S**ugar-responsive **PDE**).

From the microscale thermophoresis assay, I could measure the dissociation constant of the PdeS/c-di-GMP complex to be ~ 8.7 μM (Figure II-8), which is comparable with the Km value of PdeS toward c-di-GMP. Interestingly, however, I could not detect any interaction of c-di-GMP with PdeS in the presence of dephosphorylated $EIIA^{Glc}$, indicating that PdeS becomes inaccessible to c-di-GMP when it forms a complex with the dephosphorylated form of $EIIA^{Glc}$ (Figure II-8). Therefore, it could be assumed that the tight binding of dephosphorylated $EIIA^{Glc}$ inactivates the PDE activity of PdeS by blocking the accessibility of c-di-GMP to the active site.

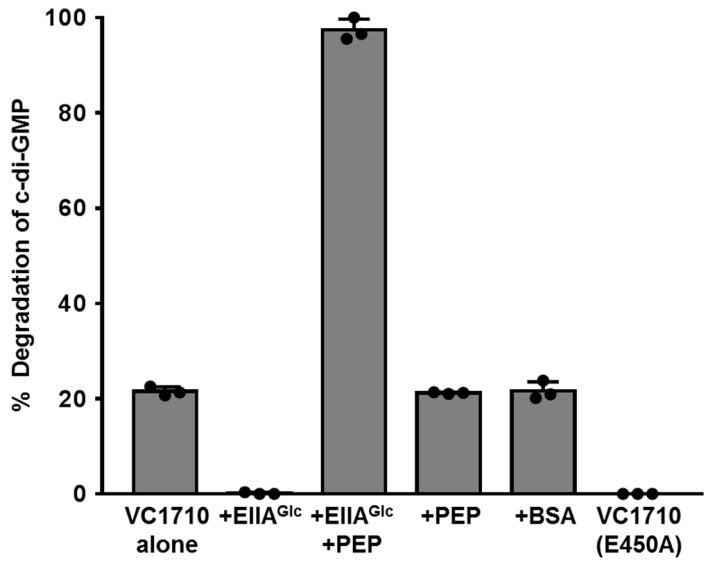

Figure II-6 Specific regulation of the c-di-GMP hydrolysis activity of VC1710 by EIIA^{Glc}.

VC1710 (1.58 μM) was mixed with 0.4 μM of EI and HPr, and its c-di-GMP hydrolysis activity was measured in the presence of different combinations of 2 mM PEP, 7.4 μM EIIA^{Glc}, and 7.4 μM BSA as indicated. The active site mutant (E450A) of VC1710 was used as a negative control of the PDE activity.

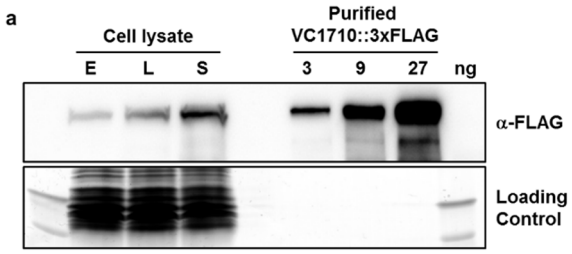

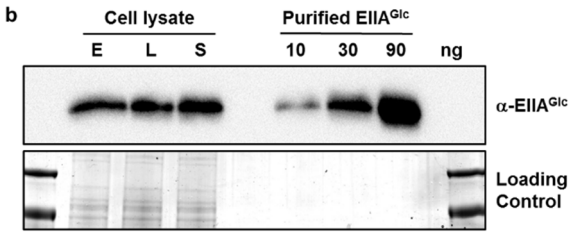

c

# of proteins	VC1710	EIIA^{Glc}
Early Exp.	29~40	17,502~21,668
Late Exp.	68~87	19,792~24,272
Stn.	126~153	22,784~30,803

Figure II-7 Quantification of EIIA^{Glc} and VC1710 in *Vibrio cholerae*.

A recombinant *V. cholerae* strain in which the chromosomal VC1710 was tagged with 3xFLAG at its C-terminus was cultured in LB medium and harvested at early exponential phase (E, OD_{600} 0.38~0.48), late exponential phase (L, OD_{600} 1.0~1.15), and stationary phase (S, OD_{600} 1.5~1.6). Cell lysates, along with purified VC1710::3xFLAG (3, 9, 27 ng) **(a)** or EIIA^{Glc} (10, 30, 90 ng) **(b)**, were electrophoresed and subjected to western blot using either α-FLAG monoclonal antibody **(a)** or α-EIIA^{Glc} anti-serum **(b)**. The amount of each protein was determined from the band intensity using ImageJ software. **c,** The cellular copy numbers of VC1710 and EIIA^{Glc} proteins were calculated assuming one *V. cholerae* cell volume of 1×10^{-15} L (Park et al., 2013a).

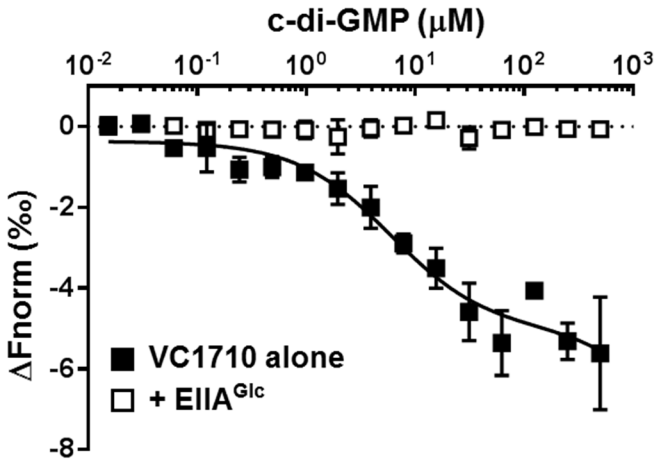

Figure II-8 Dephosphorylated EIIA^{Glc} inactivates the PDE activity of PdeS by blocking the accessibility of c-di-GMP to the active site.

The binding affinities of PdeS with c-di-GMP in the absence (black square) or presence (white square) of dephosphorylated EIIA^{Glc} were measured using NanoTemper Monolith NT.115^{pico}. An excess amount (5 μM) of EIIA^{Glc} was added to the reaction mixture to ensure all the VC1710 existed as a complex with EIIA^{Glc}. Shown are the means and SD (n=3, independent measurements).

4.3 EIIA^{Glc} regulates the activity of PdeS in vivo

To test whether PdeS can also digest c-di-GMP in the cell, I compared intracellular concentrations of c-di-GMP between the wild-type and a *pdeS*-deficient mutant strain (Δ*pdeS*) of *V. cholerae* N16961 (Fig. 3a). Because EIIA^{Glc} in cells growing in LB medium is mostly in its phosphorylated form (Figure II-13a), which stimulates the PDE activity of PdeS, the cells grown in the buffered LB medium were used to extract c-di-GMP. Measurement using LC-MS/MS revealed that Δ*pdeS* cells had an approximately 2.5 fold higher concentration of c-di-GMP than wild-type cells as expected (Figure II-9a). In addition, the Δ*pdeS* strain had a higher expression level of the Vibrio polysaccharide synthesis (*vps*) operon (Figure II-9b) and thus formed significantly more biofilm than the wild-type strain (Figure II-9a,c), which is consistent with previous reports showing that c-di-GMP induces biofilm formation (Cotter and Stibitz, 2007; Tischler and Camilli, 2004). I found that an alanine substitution mutant in the EAL domain of PdeS (PdeS(E450A)) resulted in the complete abolishment of the PDE activity (Figure II-6). While the Δ*pdeS* strain carrying an expression vector for wild-type PdeS exhibited similar levels of biofilm formation and *vps* expression with those of the wild-type strain, the mutant strain expressing PdeS(E450A) did not complement these phenotypic changes (Figure II-10). Thus, I concluded that PdeS regulates biofilm formation through its PDE activity.

Then, to confirm whether the regulation of the PdeS activity by EIIA^{Glc} also operates in *V. cholerae* cells, I constructed a dephosphomimetic mutant (H91A) of *crr* encoding EIIA^{Glc} on the chromosome and performed biofilm formation assays (Figure II-11). While I observed that the dephosphomimetic *crr* mutant showed increased biofilm formation compared to the wild-type strain, this stimulatory effect was not observed in a *pdeS* deletion mutant. EIIA^{Glc} is shared for several membrane-bound enzyme

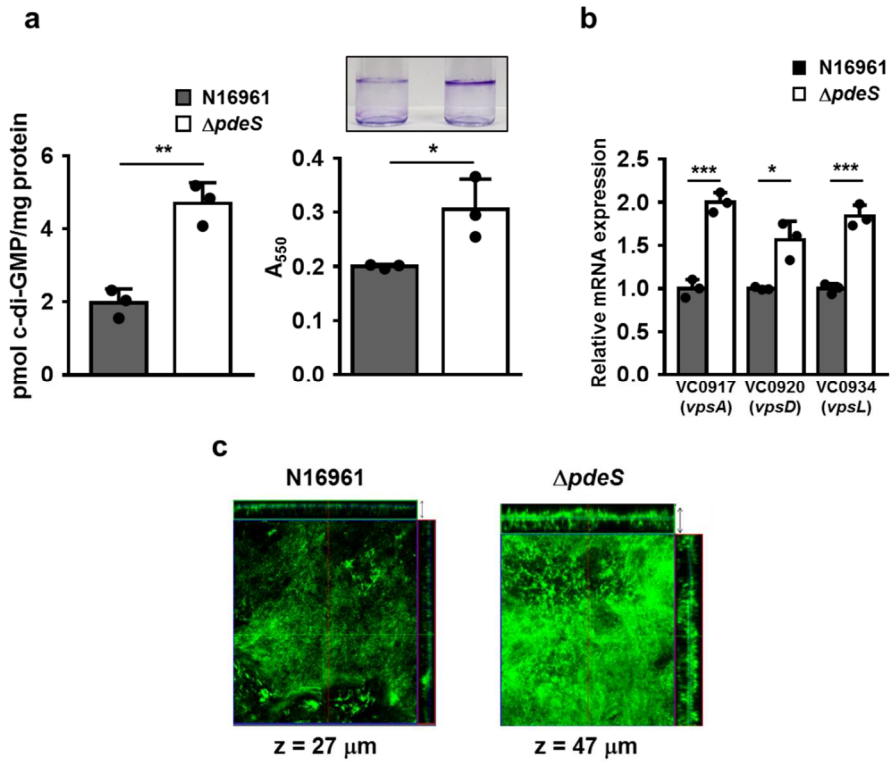

Figure II-9. PdeS regulates the c-di-GMP and biofilm formation in *V. cholerae.*

a, The intracellular c-di-GMP concentration and the biofilm-forming activity of wild-type N16961 and a Δ*pdeS* strain were measured in the buffered LB medium. The concentration of c-di-GMP extracted from the *V. cholerae* cells was determined using LC-MS/MS, and normalized with total protein contents. Biofilm formation was assessed following static growth of *V. cholerae* cells for 23 h using a crystal violet staining method62,66. The biofilm formation was determined at 550 nm. **b,** Total mRNA was isolated from the indicated strains grown in LB medium. The transcription level of genes in the *vps* cluster was measured by qRT-PCR using gene-specific primers for *vpsA*, *vpsD*, and *vpsL*. The expression values were normalized to the expression level of the *rpoB* housekeeping gene. Statistical significance was assessed using Student's t-test (p values greater than 0.05 were presented in the figure,

*p value <0.05, **p value <0.01, ***p value <0.005). Shown are the means and SD (n=3, independent measurements). **c,** Biofilm formation was visualized using confocal laser scanning microscopy. Scale bar: 50 μm

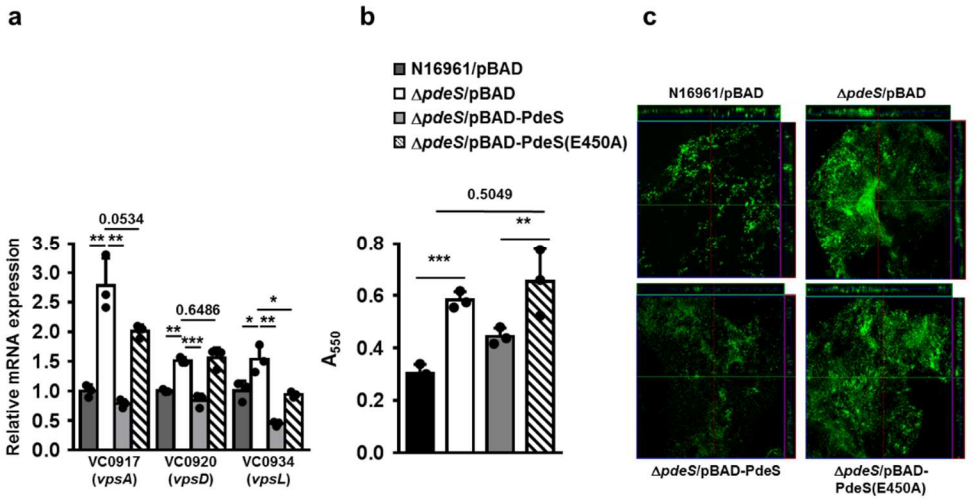

Figure II-10 PdeS modulates the intracellular c-di-GMP and thus biofilm formation.

a, Total mRNA was isolated from the indicated strains grown in LB medium containing 0.1% arabinose to induce the expression of PdeS. The transcription level of genes in the *vps* cluster was measured by qRT-PCR using gene-specific primers for *vpsA*, *vpsD*, and *vpsL*. The expression values were normalized to the expression level of the *rpoB* housekeeping gene. **b,** The biofilm-forming activity of wild-type and *pdeS* mutant *V. cholerae* strains harboring pBAD (control vector), or a pBAD-based expression vector for either wild-type PdeS or its active site mutant PdeS(E450A) was measured in LB medium containing 0.1% arabinose. Statistical significance was assessed using Student's *t*-test (*p* values greater than 0.05 were presented in the figure, **p* value <0.05, ***p* value <0.01, ****p* value <0.005). Shown are the means and SD (n=3, independent measurements). **c,** Biofilm formation was visualized using confocal laser scanning microscopy. Scale bar: 50 μm

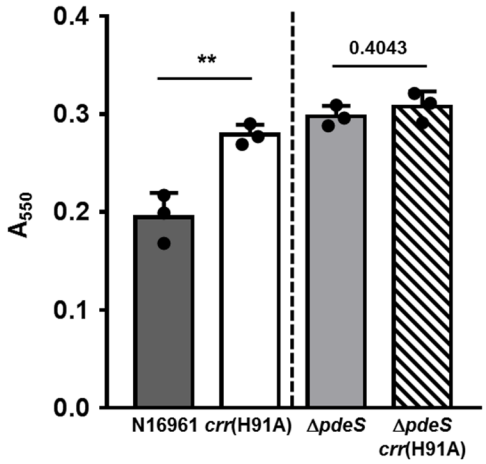

Figure II-11 Regulation of biofilm formation by EIIA^{Glc} is dependent on PdeS.

The biofilm formation by the wild-type *V. cholerae* N16961 strain and its derivatives carrying *crr*(H91A) and/or *pdeS* mutations was quantified. Statistical significance was assessed using Student's *t*-test (*p* values greater than 0.05 were presented in the figure, ***p* value <0.01). Shown are the means and SD (n=3, independent measurements).

IIBCs including those specific for glucose, *N*-acetylglucosamine, sucrose, and trehalose in *V. cholerae* and phosphorylatable $EIIA^{Glc}$ is indispensable for a variety of physiological processes including the regulation of global transcription factors such as CRP and Mlc. Therefore, I assume that the phenotype of this chromosomal *crr* mutant might be due to indirect pleiotropic effects of the mutation. For this reason, I tried to see the effect of $EIIA^{Glc}$ dephosphorylation on biofilm formation by increasing the level of the dephosphomimetic mutant of $EIIA^{Glc}$ while minimizing the perturbation of the overall PTS activity. Therefore, I compared biofilm formation and the intracellular level of c-di-GMP of the wild-type strain carrying an expression vector for wild-type $EIIA^{Glc}$ with the wild-type strain carrying an expression vector for $EIIA^{Glc}$(H91A), and observed increased biofilm formation and the c-di-GMP level in the latter strain (Figure II-12), which is in accordance with the result obtained by the chromosomal mutation of the *crr* gene. Together my data show that dephosphorylated $EIIA^{Glc}$ inactivates the PDE activity of PdeS and thereby increases the c-di-GMP level in vivo. Thus, it could be assumed that $EIIA^{Glc}$ can modulate biofilm formation by controlling the c-di-GMP level through direct interaction with PdeS.

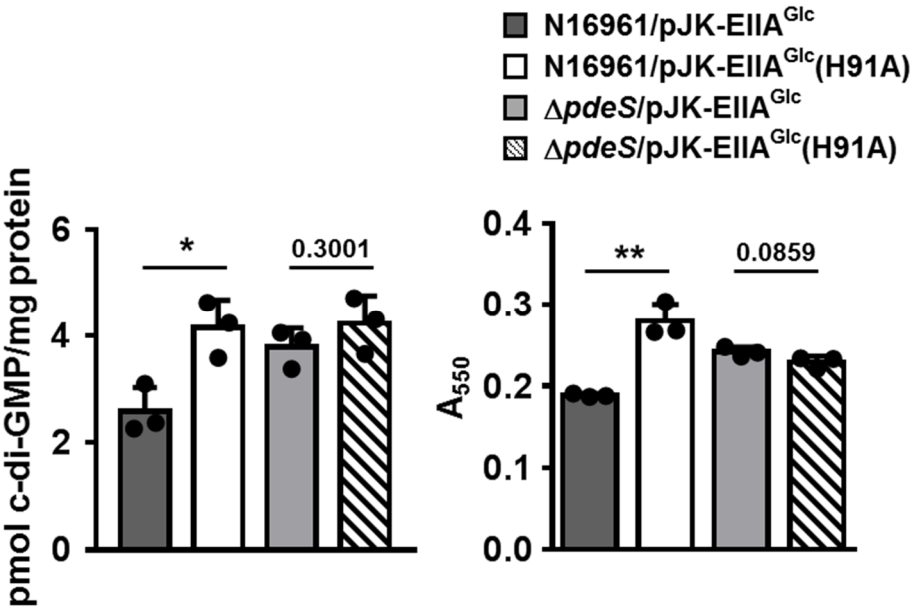

Figure II-12. PdeS regulates the intracellular concentration of c-di-GMP and biofilm formation depending on the phosphorylation of EIIA^{Glc}.

The effect of EIIA^{Glc} on the c-di-GMP hydrolysis activity of PdeS was assessed *in vivo*. The intracellular c-di-GMP concentration and the biofilm-forming activity of wild-type and Δ*pdeS V. cholerae* strains harboring a pBAD-based expression vector for either wild-type EIIA^{Glc} or dephosphomimetic mutant EIIA^{Glc}(H91A) were determined in the presence of 0.1% arabinose. Statistical significance was assessed using Student's *t*-test (*p values* greater than 0.05 were presented, **p* value <0.05, ***p* value <0.01). Shown are the means and SD (n=3, independent measurements).

4.4 EIIA^{Glc} regulates biofilm formation depending on carbon sources.

PTS components including EIIA^{Glc} can have a different phosphorylation state depending on the availability of PTS substrates. As the PDE activity of PdeS and thus the intracellular concentration of c-di-GMP are modulated depending on the phosphorylation state of EIIA^{Glc}, I examined whether biofilm formation can be influenced by carbohydrates encountered by *V. cholerae* in their environmental niches. Thus, I performed a biofilm formation assay in the presence of various carbon sources in LB medium. To exclude the effect of the pH decrease due to fermentation of sugar, I buffered LB medium with 40 mM potassium phosphate, pH 7.0. At the same time, I determined the in vivo phosphorylation state of EIIA^{Glc} in each medium (Fig. II-13a). Consistent with previously reported results in *E. coli* and *V. vulnificus* (Nam et al., 2005; Park et al., 2016), EIIA^{Glc} was mostly dephosphorylated in glucose-containing medium, while mostly phosphorylated in LB medium without additional carbon source. I could also find a significant positive correlation between the degree of EIIA^{Glc} phosphorylation and the inhibitory effect of PdeS on biofilm formation (Figure II-13b). These data imply that the modulation of biofilm formation by PdeS is dependent on the phosphorylation state of EIIA^{Glc}, which is determined by the environmental carbon source.

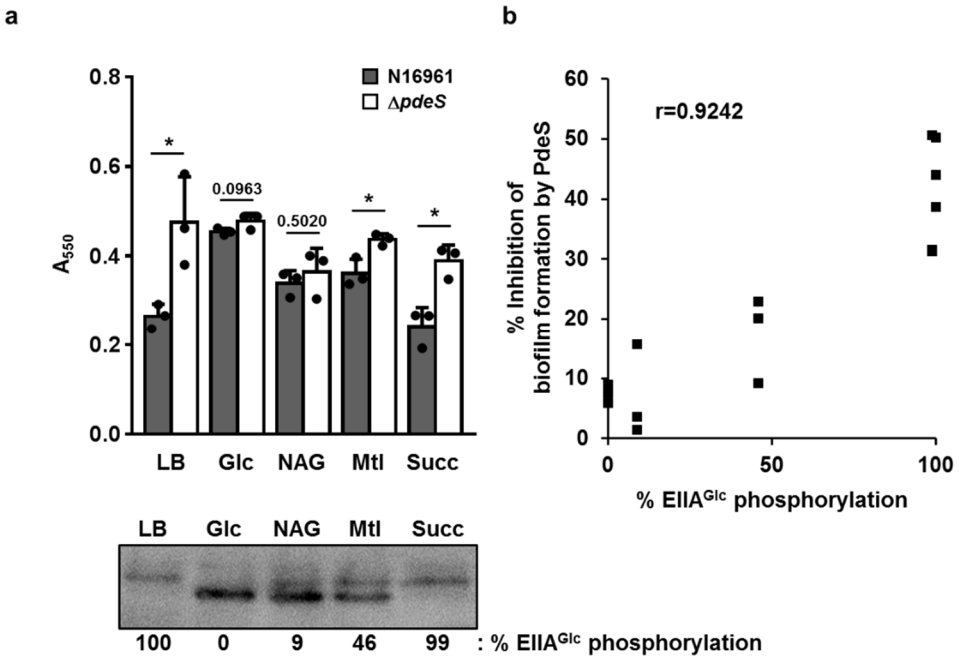

Figure II-13 PdeS regulates biofilm formation depending on carbon sources.

a, The level of biofilm formation was compared between wild-type N16961 and a Δ*pdeS* strain in the presence of various carbon sources in buffered LB medium. At the same time, the phosphorylation state of $EIIA^{Glc}$ was determined by western blot using anti-$EIIA^{Glc}$ mouse serum after SDS-PAGE. Statistical significance was assessed using Student's t-test (**p* value <0.05, *p* values greater than 0.05 were presented). Glc, glucose; NAG, N-acetylglucosamine; Mtl, mannitol; Succ, Succinate. **b,** The inhibitory effect of PdeS on the biofilm formation was plotted as a function of $EIIA^{Glc}$ phosphorylation. Based on the data in panel a, the degree of biofilm formation of wild-type cells was divided by that of the Δ*pdeS* mutant cells. The percentage of biofilm formation inhibition by PdeS was then calculated by subtracting the resultant value from 1 and multiplying by 100, then plotted as a function of the percentage of phosphorylated $EIIA^{Glc}$ over total $EIIA^{Glc}$. The correlation between the sugar-mediated phosphorylation state of $EIIA^{Glc}$ and

biofilm formation was assessed using Pearson's correlation coefficient ($r = 0.9242$, $p < 0.005$).

4.5 EIIA^{Glc} regulates biofilm formation and host gut colonization.

V. cholerae is associated with various hosts, including arthropods, insect eggs, and unicellular eukaryotes as well as humans (Butler and Camilli, 2005). Recently, the interaction between *V. cholerae* and the fruit fly *Drosophila melanogaster* has been intensively studied, since this arthropod model acts as a disease reservoir in nature (Blow et al., 2005) and is also simple but has similar physiological features and anatomical structures with mammalian infection models (Mistry et al., 2016). It has been reported that Vibrio exopolysaccharide (VPS)-dependent biofilm formation is indispensable for attachment and colonization in the *Drosophila* intestine in a quorum sensing-defective *V. cholerae* strain (Kamareddine et al., 2018; Purdy and Watnick, 2011). Therefore, I assumed that VPS might also play a critical role in the intestinal colonization in the N16961 strain which carries a natural frame-shift mutation in the *hapR* gene encoding the quorum-sensing master regulator HapR. As the expression of the *vps* operon was controlled by c-di-GMP, which is the substrate of PdeS, I assumed that PdeS might also play a role in the regulation of intestinal colonization. Since mannitol transport by *V. cholerae* requires mannitol-specific EII but not EIIA^{Glc} in spite of its structural similarity with glucose, the phosphorylation state of EIIA^{Glc} is different in the presence of the two PTS sugars (Figure II-13a). Therefore, I chose glucose and mannitol as representative sugars leading to dephosphorylation and ~50% phosphorylation of EIIA^{Glc}, respectively, to evaluate the EIIA^{Glc} phosphorylation state-dependent regulation of the colonization efficiency of *V. cholerae*. To investigate whether a sugar-dependent change in EIIA^{Glc} phosphorylation influences bacterial colonization in the intestine through the modulation of PdeS activity, flies were fed 5% sugar (glucose or mannitol) solution containing ~10^6 cells μl^{-1} of the *V. cholerae* N16961 strain for 24 h, and subsequently fed the same sugar

solution without bacteria for 9 h. These flies were then surface-sterilized, homogenized in 1 ml of PBS buffer and spread on an agar plate for the quantification of the colonization of *V. cholerae* in vivo by measuring colony forming units (CFUs). While the CFU of the Δ*pdeS* strain was not affected by the sugar source, the CFU of the wild-type strain was significantly lower in flies fed mannitol compared to flies fed glucose (Figure II-14a). In flies fed mannitol, the wild-type strain gave significantly lower CFU levels compared to the Δ*pdeS* strain. Therefore, I could assume that, in the presence of mannitol, phosphorylated $EIIA^{Glc}$ stimulates the PdeS activity to decrease the c-di-GMP level and thereby biofilm formation.

To determine whether the effect of PdeS on intestinal colonization is mediated by the regulation of biofilm formation, I repeated the colonization experiment with Δ*vpsA* and Δ*vpsA pdeS* mutants (Figure II-14a). As reported previously (Kamareddine et al., 2018; Purdy and Watnick, 2011), mutation of *vpsA* resulted in a significantly reduced (~5%) intestinal colonization in flies compared to the wild-type strain. Interestingly, the inhibitory effect of PdeS on intestinal colonization was not seen in this *vpsA* mutant strain. Thus, it could be assumed that VPS-dependent biofilm formation is important for the regulation of intestinal colonization by PdeS.

Then, to assess whether PdeS affects the earlier stage of *V. cholerae* infection of the *Drosophila* intestine, I infected flies orally with 5% sugar solution containing ~10^8 cells μl^{-1} of wild-type *V. cholerae* N16961 or its *pdeS* mutant for 2 h. After feeding flies with bacteria-free 5% sugar solution for another 2 h and surface sterilization, I quantified the intestinal colonization of *V. cholerae* by measuring CFUs (Figure II-14b). While the CFU of the Δ*pdeS* strain showed no difference depending on the sugar source, the CFU of the wild-type strain was significantly lower in flies fed mannitol compared to flies fed glucose. Therefore, my data indicates that PdeS may regulate the

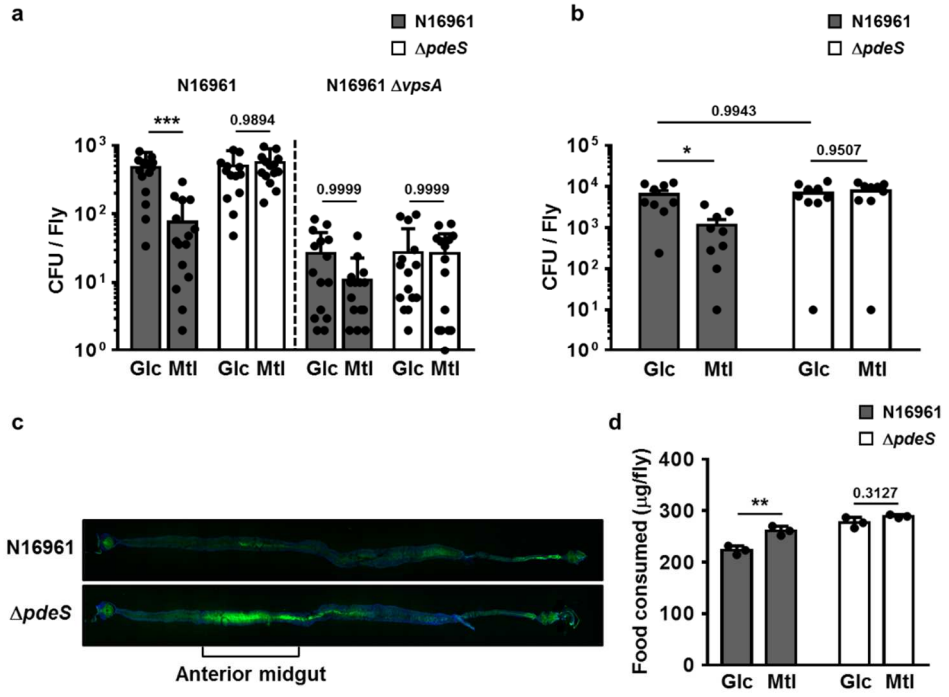

Figure II-14 PdeS regulates intestinal colonization depending on the host diet.

a, Flies were orally administered a 5% sugar solution containing the indicated *V. cholerae* strains for 24 h, and fed a sterile sugar solution for another 9 h. The homogenate of the surface-sterilized fly was spread on a selective medium for *V. cholerae* and colony forming units (CFU) were measured. **b,** Intestinal colonization was assessed for a shorter infection period. Flies were orally administered a 5% sugar solution containing the indicated *V. cholerae* strains for 2 h, and fed a sterile sugar solution for another 2 h. **c,** The *V. cholerae* colonization on the alimentary canal was visualized using confocal laser scanning microscopy. Flies were exposed to *V. cholerae* strains harboring a GFP expression vector in the presence of 5% mannitol for 2 h and, after incubation in a sterile medium for another 2 h, the whole intestines were dissected and visualized. Shown are the representative images from three

independent experiments on different days. Scale bar: 500 μm **d,** Food consumption was measured by dye uptake using FD&C Blue #1 dye during bacterial infection (Ha et al., 2009). Shown are the means and SD (n=6, independent measurements). Data was analyzed using a two-way ANOVA followed by Tukey's post hoc test (*p value <0.05, ***p value <0.005, p values greater than 0.05 were presented).

initial phase of intestinal colonization of *V. cholerae*.

To determine which compartment(s) *V. cholerae* colonizes and to examine the physiological relevance of the host diet-dependent colonization, flies were exposed to the *V. cholerae* N16961 strain carrying a GFP expression vector in the presence of 5% mannitol, and their colonization on the wholealimentary canal was visualized (Figure II-14c). Although the amounts of ingested bacteria (as estimated by the ingested amounts of bacteria-containing sugar solutions) were similar between wild-type and Δ*pdeS* strains (Figure II-14d), more intensive colonization was detected in flies infected with the Δ*pdeS* strain than in flies infected with the wild-type strain, especially in the anterior midgut, which is the main site of digestion and nutrient absorption in my infection condition (Figure II-14c). This result is consistent with the CFU data (Figure II-14b), implying that PdeS modulates the colonization efficiency of *V. cholerae* depending on the host diet, which is consistent with its sugar-dependent regulation of c-di-GMP and biofilm formation.

5. Discussion

The pathogen *Vibrio cholerae*, like other bacteria, has various niches including natural seawater, copepod, chironomid egg masses, and the human host (Butler and Camilli, 2005). The ability to sense and respond to each environment is the crucial factor for adaptation and propagation of bacteria. In many bacteria, the PTS is one of the sensory systems that regulate multiple metabolic pathways in response to the availability of carbon or nitrogen nutrients in diverse environments (Postma et al., 1993). Previous studies suggested that the PTS in *V. cholerae* also has regulatory functions in biological processes such as biofilm formation (Houot and Watnick, 2008; Pickering et al., 2012), colonization in the mammal host (Houot et al., 2010a), chitin utilization and natural competence (Blokesch, 2012). Because most of these regulations are mediated by protein-protein interactions (Deutscher et al., 2014b), the characterization of the interaction network of the PTS is vital for understanding the orchestrated cellular responses to environmental changes. In this study, I found a new interaction partner of $EIIA^{Glc}$, the c-di-GMP phosphodiesterase PdeS which hydrolyzes the ubiquitous bacterial second messenger c-di-GMP. As the c-di-GMP signaling pathway is involved in many behaviors such as biofilm formation, motility, and toxin production, this interaction is expected to be an important key to reveal many nutrient-related phenotypes.

Many studies suggested that c-di-GMP induces the transition from motile to sessile mode by binding to and regulating various receptors involved in biofilm formation (Beyhan et al., 2007; Ryjenkov et al., 2006). Biofilm matrix serves as a barrier against various environmental stresses, which enables bacteria to prosper as long as sufficient nutrients are available. However, once nutrients become scarce, bacterial cells detach and disperse from this community by reducing the production of this polymeric matrix. Several

studies have reported that nutrient deprivation decreases biofilm formation and induces biofilm dispersion by decreasing intracellular c-di-GMP (Gjermansen et al., 2005; Sauer et al., 2004; Schleheck et al., 2009). The interaction between $EIIA^{Glc}$ and PdeS is expected to be one of these regulatory mechanisms.

It is notable that modulation of c-di-GMP hydrolytic activity of PdeS by $EIIA^{Glc}$ is comparable to the regulation of cAMP synthetic activity of adenylate cyclase (Park et al., 2006). In several bacteria, only the phosphorylated form of $EIIA^{Glc}$ is known to stimulate cAMP synthesis (Deutscher et al., 2014b; Park et al., 2016; Park et al., 2006). Similarly, my data in this study show that dephosphorylated $EIIA^{Glc}$ strongly inhibits c-di-GMP hydrolysis, whereas its phosphorylated form stimulates c-di-GMP hydrolysis in *V. cholerae*. The copy number of the $EIIA^{Glc}$ protein was reported to be 20,000~30,000, while that of adenylate cyclase to be less than 10 in *E. coli* (Schmidt et al., 2016). According to my analytical western blot results, the copy number of $EIIA^{Glc}$ in a *V. cholerae* cell was estimated to be similar to that in *E. coli* and that of the PdeS protein to be 29~153 (Figure II-7). Because the number of $EIIA^{Glc}$ is significantly higher than that of PdeS and adenylate cyclase, $EIIA^{Glc}$ appears to simultaneously control the amount of c-di-GMP and cAMP, yet in the opposite direction, in *V. cholerae*. As the cAMP-CRP complex has been reported to inhibit biofilm formation by differentially regulating the expression of several c-di-GMP metabolizing enzymes (Fong and Yildiz, 2008; Liang et al., 2007), it was expected that the cAMP pathway would mitigate the regulatory effect of PdeS on biofilm formation. However, the expression level of PdeS was not changed by the sugar type (Figure II-15). Moreover, the PdeS-mediated regulation of biofilm formation was quantitatively correlated to the phosphorylation state of $EIIA^{Glc}$ (Figure II-13). Therefore, I concluded that although the intracellular

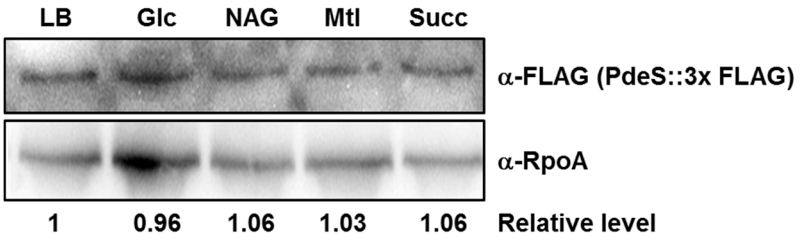

Figure II-15 Effect of carbon sources on PdeS expression.

The level of PdeS protein was determined in a *V. cholerae* strain in which the chromosomal PdeS was tagged with 3xFLAG at its C-terminus grown in LB medium or LB medium supplemented with the indicated carbon sources at OD_{600} ~1.0. Cell lysates were analyzed by western blot using α-FLAG monoclonal antibody. The level of PdeS was determined by measuring the band intensity using ImageJ software followed by normalization with that of RNA polymerase α subunit (RpoA). The levels of PdeS were expressed relative to that of PdeS in LB medium, which was set to 1. Glc, glucose; NAG, N-acetylglucosamine; Mtl, mannitol; Succ, succinate.

level of cAMP and c-di-GMP was controlled at the same time, the sugar-dependent c-di-GMP regulatory pathway is hardly affected by the cAMP signaling pathway in *V. cholerae* N16961. In addition, it could be assumed that the indirect interplay between the cAMP and c-di-GMP signaling pathways might play only a minor role, if any, in the sugar-dependent regulation of biofilm formation in this strain. In previous studies, different effects of cAMP-CRP on biofilm formation have been reported among various *V. cholerae* strains. While biofilm formation was negatively regulated by the cAMP-CRP complex in the C1552 and C6728 strains (Fong and Yildiz, 2008; Liang et al., 2007), the supplementation of the growth medium with various concentrations of cAMP had no effect on the total growth and biofilm accumulation by a crr mutant of the MO10 strain28. Herein, I report that the sugar-dependent regulation of biofilm formation is not affected by cAMP-CRP in the N16961 strain. This may simply be the result of strain differences, as *V. cholerae* is known to undergo genetic drift in laboratory culture (Stutzmann and Blokesch, 2016)53.

During the host infection, the intracellular concentration of c-di-GMP in *V. cholerae* is changed along its infection stage54. Also, the c-di-GMP pool fluctuates in response to various external signals, choosing the fittest infection strategy depending on the environmental condition55. Thus, the sophisticated regulation of c-di-GMP contents appears to be a prerequisite for a successful propagation and transmission to new hosts throughout the infection cycle. In this respect, my findings provide a new insight into how pathogenic bacteria cope with fluctuating nutritional conditions including those encountered during passage through the intestinal tract of the host (Figure II-16).

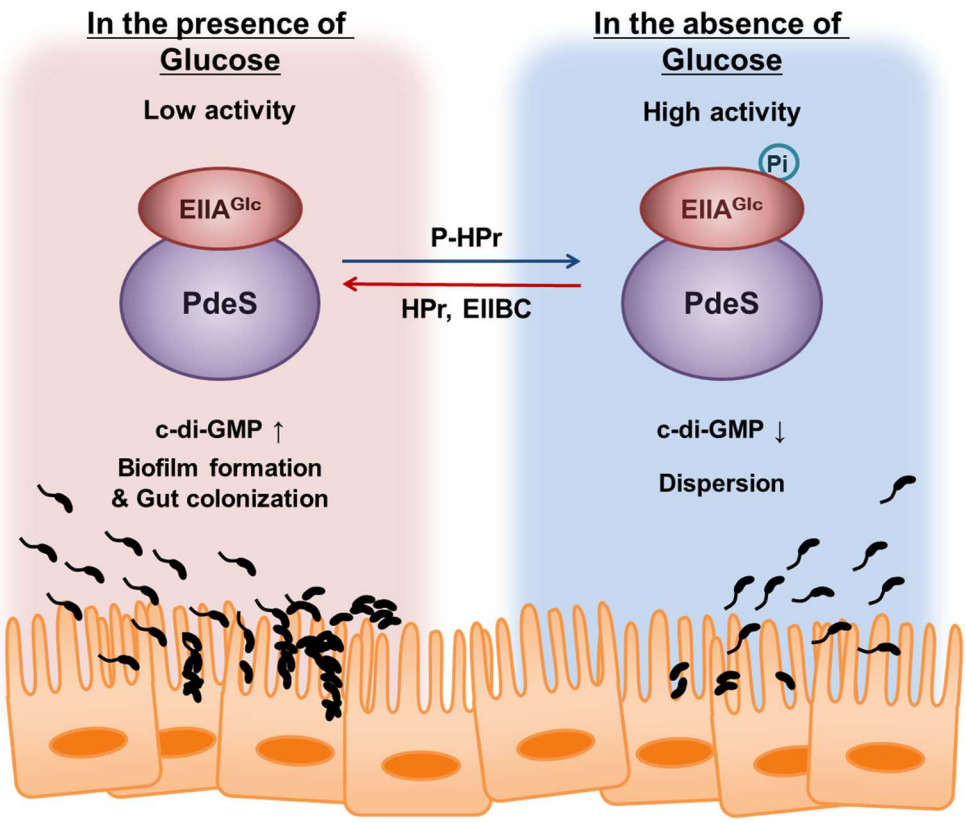

Figure II-16 Schematic model of how EIIA^{Glc} modulates the c-di-GMP level and biofilm formation in the infection stage.

Chapter III. A novel flux-dependent regulation of lysine acetyltransferase in *Escherichia coli*

1. Abstract

The primary concern of bacteria is sensing the availability and quality of nutrients in their environments, and redirecting metabolic flux between the catabolic and anabolic pathway in response. Thus, it is assumable that bacteria possess the sophisticated sensory mechanisms of a variety of metabolic changes in the environment. It has been suggested that the signal transduction system responding to the metabolic fluxes is an efficient way to adapt environment fluctuations in the presence of various nutritional input, instead of responding to each extracellular stimulus respectively. However, difficulties lie in seeking the representative metabolite that store the flux information in their concentration becomes an obstacle to identify a novel flux-dependent signal transduction system. In this study, I suggest that malate dehydrogenase, the last enzyme in tricarboxylic acid cycle, and its cofactor NADH act as a flux-dependent signal transduction system sensing the quality of carbon source. Through the inhibition of the activity of a lysine acetyltransferase PatZ in NADH-dependent manner, malate dehydrogenase may potentially participate in the metabolic adaptation in *Escherichia coli*.

2. Introduction

Bacteria sense and adapt to extracellular changes, such as metabolic fluctuations (Gerosa and Sauer, 2011; Kochanowski et al., 2013). These biological responses and adaptations to environmental stimuli directly occur through various signal transduction systems including two-component system (Stock et al., 2000). In addition, it has been reported that microorganisms also exhibit phenotypic changes upon intracellular alterations of metabolic flux rates or metabolite level independent of extracellular changes (Kochanowski et al., 2013; Okano et al., 2020). For example, in *E. coli*, carbon sources transported and metabolized sequentially in batch cultures are simultaneously utilized in the continuous cultures (Lendenmann et al., 1996). Also, *E. coli* exhibits differentiated gene expression and proteome profiles under altered flux rates and growth limitation (Basan et al., 2015). Considering that such a way for sensing and transducing flux signal is regulated by the actual metabolic status of the cells instead of the identity of the nutrient sources, this system is expected to be well conserved in wide range of species from bacteria to higher organisms(Gerosa and Sauer, 2011; Litsios et al., 2018). However, a few examples have been reported.

The prerequisite for the flux-dependent signal transduction system is the assessment of metabolic flux, which is generally determined by the intracellular concentration of representative metabolites, called “flux-signaling metabolites” (Litsios et al., 2018). Thus, it has been thought that the level of flux-signaling metabolite needs to correlate with the cognate metabolic flux so that it could store the flux information in its concentration. Also, effectors would be macromolecules which can interact with the metabolites and transduce the flux information in a concentration-dependent manner.

Malate dehydrogenase, the last enzyme of tricarboxylic acid cycle (TCA), catalyzes the interconversion between malate and oxaloacetate using NAD^+ or NADH as a cofactor. Although malate dehydrogenase exhibits larger K_m value against malate and NAD^+ than oxaloacetate and NADH in most bacteria, malate dehydrogenase generally catalyzes the oxidation of malate for net free energy in the cell. Thus, once intracellular NADH is accumulated, or cells are exposed to the oxidative stress, malate dehydrogenase can easily shift the direction of reaction it catalyzes and participate in the reductive TCA cycle (Chakraborty et al., 2020; Shimizu and Matsuoka, 2019). In this perspective, I thought that malate dehydrogenase can act as a flux sensor of the abnormal shift in intracellular concentration of oxaloacetate or NADH.

In this study, I found that malate dehydrogenase interacts with PatZ, a lysine acetyltransferase in the manner dependent on the concentration of NADH. When bacterial metabolism is mainly through respiration, malate dehydrogenase inhibits the the activity of PatZ and changes the acetylation pattern of target metabolic enzymes, resulting in the modification of metabolic flux. Finally, I propose tha this interaction may function as a flux-dependent signal transduction systems that involved in the bacterial metabolic adaptation.

3. Materials & Methods

3.1 Strain

The bacterial strains and plasmids used in this study are listed in Supplementary Table 2. *E. coli* strains were cultured in Luria-Bertani medium or M9 minimal medium supplemented with the indicated carbon sources.

3.2 Purification of overexpressed proteins

Proteins (His-Mdh, PatZ-His) were expressed in *E. coli* ER2566 by adding 1 mM IPTG. His-tagged proteins were purified using TALON metal-affinity resin (Takara Bio.) according to the manufacturer's instructions. His-tagged proteins were eluted with 200 mM imidazole and the fractions containing His-tagged proteins were pooled and concentrated using Amicon Ultracel-3K centrifugal filters (Merck Millipore). To increase the purity of proteins and remove imidazole, the concentrated pool was chromatographed on a Hiload 16/60 Superdex 200 pg column (GE Healthcare) equilibrated with buffer A (25 mM HEPES-NaOH (pH 7.6), containing 200 mM NaCl, 10 mM β-mercaptoethanol).

3.3 Ligand fishing using metal affinity resin

Ligand-fishing experiments were performed as described previously with minor modifications to find a new interaction partner of HisMdh. *Escherichia coli* K-12 MG1655 cells grown at 37 ˚C overnight at LB (200 ml) were harvested and resuspended in buffer A. Cells were then disrupted by three passages through a French pressure cell at 8,000 psi. After centrifugation at 10,000 x g for 20 min at 4 ˚C, the supernatant was mixed with 150 μg of His-Mdh or buffer A as control in the presence of TALON metal affinity resin in

a 15-ml tube, then incubated at 4 ˚C for 30 min. After brief washes with buffer A containing 10 mM imidazole, the bound proteins were eluted with buffer A containing 200 mM imidazole and analyzed by SDS-PAGE using a 4-20% gradient Tris-glycine gel (KOMA biotech) and staining with Coomassie brilliant blue R. Protein bands specifically bound to the His-tagged bait protein were excised from the gel, and in-gel digestion and peptide mapping of the tryptic digests were performed using MALDI-TOF MS.

3.4 Determination of intracellular concentration of metabolites.

E. coli was cultivated in LB medium (200 ml) to OD_{600} ~1.0, and centrifuged at 4,000 x g for 10 min. The cell pellet was washed twice with 30 ml M9 minimal medium and resuspended in 10 ml M9 minimal medium supplemented with the indicated carbon sources. After incubation at 37 ˚C for 1 h the cells were centrifuged and the cell pellet was resuspended in 500 μl of extraction buffer (40% methanol, 40% acetonitrile, and 0.1 N formic acid) and incubated on ice for 15 min. Each sample was subjected to three cycles of freezing/thawing using -80 ˚C freezer and heat block adjusted to 50 ˚C. After an additional 15-min incubation on ice, the sample was centrifuged at 16,100 x g for 10 min, and 400 μl of the supernatant was dried under vacuum. The lyophilized metabolites were resuspended in 80 μl of 100% methanol, followed by quantification using LC-MS/MS

3.5 Acetylation assay

In vitro acetylation activity was determined by immuno-detecting and quantifying acetylated proteins after reactions using anti-acetyllysine antibody (Venkat et al., 2017). The reaction contained 50 mM Tris-HCl (pH

8.0), 50 mM NaCl, 1 mM DTT, 1 mM Acetyl-coA and 1 μM purified Strep-tagged acetyl-coA synthetase in addition to purified PatZ in a total volume of 50 μl. To assess the effect of Mdh on acetylation activity of PatZ, I added 20 μM of purified HisMdh to the reactions in the presence of 2 mM NAD^+ or NADH. The enzymatic reaction was started by the addition of 1 mM Acetyl-coA and allowed to proceed at 37 ˚C for 1 h. Reactions were stopped by adding SDS buffer and boiling for 5 min. A 20-μl aliquot of each sample was then resolved by SDS-PAGE using a 12% Tris-glycine gel, and acetylated proteins was visualized by western blot using anti-acetyllysine antibody.

3.6 Determination of malate dehydrogenase activity

The bidirectional activity of malate dehydrogenase was determined by continuous measurement of the produced or remaining NADH. The reaction contained 20 mM Tris-HCl (pH 8.0), 50 mM NaCl, 5 mM $MgCl_2$, 5 mM β-mercaptoethanol, 3 nM purified malate dehydrogenase, 0.5 mM NAD^+, and 15 mM malate (or 0.2 mM NADH and 0.3 mM oxaloacetate). The produced NADH in the malate oxidation is simultaneously oxidized by a second electron acceptor PMS and it converts *p*-iodonitrotetrazolium violet (INT) to red formazan, which is monitored at 500 nm. The remaining NADH in the reaction from conversion of oxaloacetate to malate is monitored at 340 nm.

Table III-1. Bacterial strains and plasmids used in this study

Strain or Plasmid	Genotype or phenotype	Source
Strains		
MG1655	Wildtype	
MG1655 Δ*patZ*	MG1655 with Δ*patZ*	This study
MG1655 Δ*ptsG*	MG1655 with Δ*ptsG*	This study
MG1655 Δ*ptsG patZ*	MG1655 with Δ*ptsG patZ*	This study
Plasmids		
pETDuet-1		Novagen
pET-HisMdh	pETDuet-1-based expression vector for His-Mdh, Amp^r	This Study
pET-PatZ	pETDuet-1-based expression vector for PatZ, Amp^r	This Study
pET-StrepAcs	pETDuet-1-based expression vector for StrepAcs, Amp^r	This Study
pGEX-PatZ	pGEX4t1-based expression vector for GST tagged PatZ, Amp^r	This Study

4. Results

4.1 Malate dehydrogenase interacts with a lysine acetyltransferase in *Escherichia coli.*

To investigate an additional role of malate dehydrogenase, I performed ligand fishing experiments using hexahistidine-tagged Mdh (HisMdh) as a bait. Crude extracts prepared from *Escherichia coli* MG1655 cells grown overnight in LB medium were mixed with TALON metal affinity resin in the presence and absence of HisMdh. After several washes, total proteins bound to resins were eluted with buffer containing 200 mM imidazole. Repeated analysis of the eluted proteins by SDS-PAGE followed by staining with Coomassie brilliant blue R, revealed dramatic enrichment of a protein band with molecular mass of approximately 90 kDa in the fraction containing HisMdh (Figure III-1). MALDI-TOF mass spectrometry and peptide fingerprinting revealed that this band corresponded to PatZ, one of the lysine acetyltransferases. Lysine acetyltransferases including PatZ catalyze the acetylation on specific lysine residues of various proteins involved in metabolism, motility and RNA stability by using acetyl coenzyme A (AcCoA) as an acetyl donor (Castano-Cerezo et al., 2014; de Diego Puente et al., 2015; Starai and Escalante-Semerena, 2004). Thus, I assumed that the interaction between malate dehydrogenase and PatZ could be a novel flux-dependent signal transduction system that mediates variety of phenotypic changes.

To validate the ligand-fishing data, I repeated ligand fishing experiment using cell extracts from wild-type *E. coli* MG1655 and its isogenic *patZ* deletion mutant (Δ*patZ*) (Figure III-2a). While I found the enriched PatZ band in the set with wild-type *E. coli* cell crude, the PatZ band was barely detectable in the sample incubated with the Δ*patZ* extract (Figure III-2a). Also, when *E. coli* cell extracts expressing recombinant PatZ was mixed with

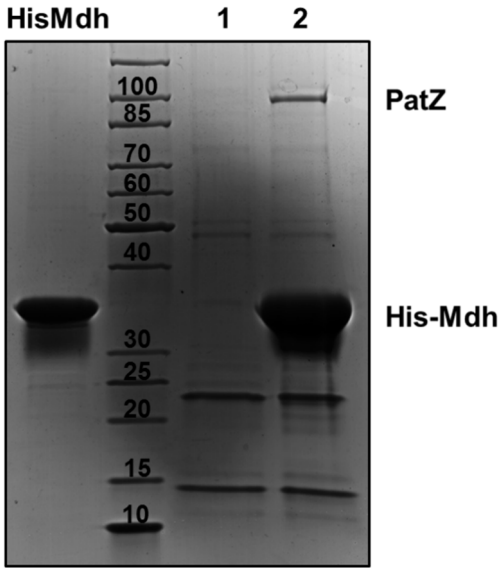

Figure III-1. Malate dehydrogenase binds to a lysine acetyltransferase in *E. coli*

Ligand fishing experiment was carried out to find proteins interacting with HisMdh. Crude extract prepared from *E. coli* MG1655 cells was mixed with buffer A (lane 1) or 150 μg of purified HisMdh (lane 2). Each mixture was subjected to TALON metal affinity chromatography and proteins bound to the column were analyzed as described in Materials and Methods.

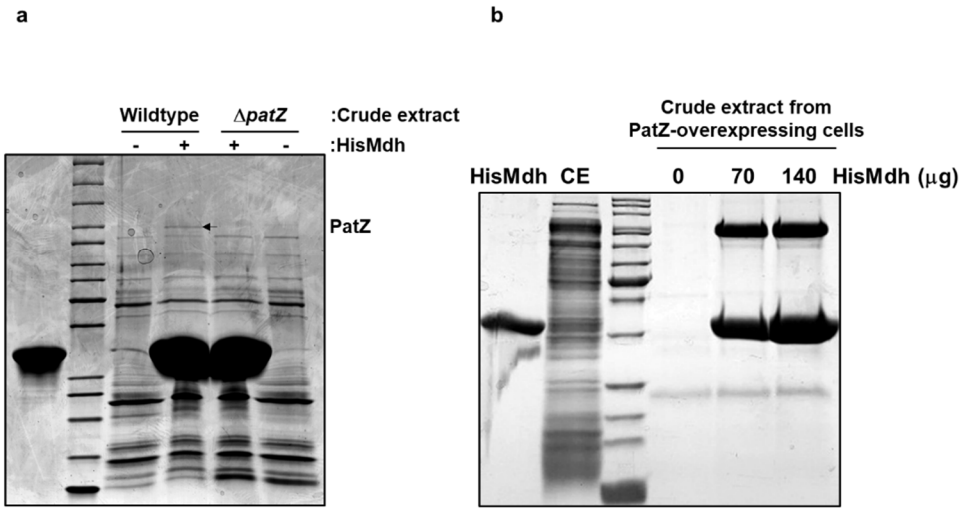

Figure III-2. Malate dehydrogenase specifically interacts with PatZ

a, Crude extract prepared from wild-type and its isogenic *patZ* deletion mutant (Δ*patZ*) of *E. coli* MG1655 cells was mixed with buffer A or 150 μg of purified HisMdh. Each mixture was subjected to TALON metal affinity chromatography and proteins bound to the column were analyzed. **b,** *E. coli* cell lysate expressing recombinant PatZ (lane CE) was mixed with buffer A or increasing amount of HisMdh and subjected to TALON metal affinity chromatography as in panel a.

increasing amounts of HisMdh and subjected to TALON metal affinity chromatography, a concentration-dependent interaction of PatZ was observed, confirming the specific interaction between Mdh and PatZ (Figure III-2b).

Malate dehydrogenase catalyzes the bidirectional reaction between malate and oxaloacetate using NAD^+ or NADH as a cofactor. To assess whether the bindings of these four ligands could affect the interaction between Mdh and PatZ, I performed ligand fishing experiments in the presence of either 2 mM NAD^+ or NADH or in the presence of either 2 mM malate or oxaloacetate (Figure III-3). In repeated experiments, PatZ was co-eluted with HisMdh as previous ligand-fishing results, yet only in the set incubated with NADH. These results suggested that intracellular concentration of NADH or NADH/NAD^+ ratio could act as a signal molecules modulating the interaction between malate dehydrogenase and PatZ.

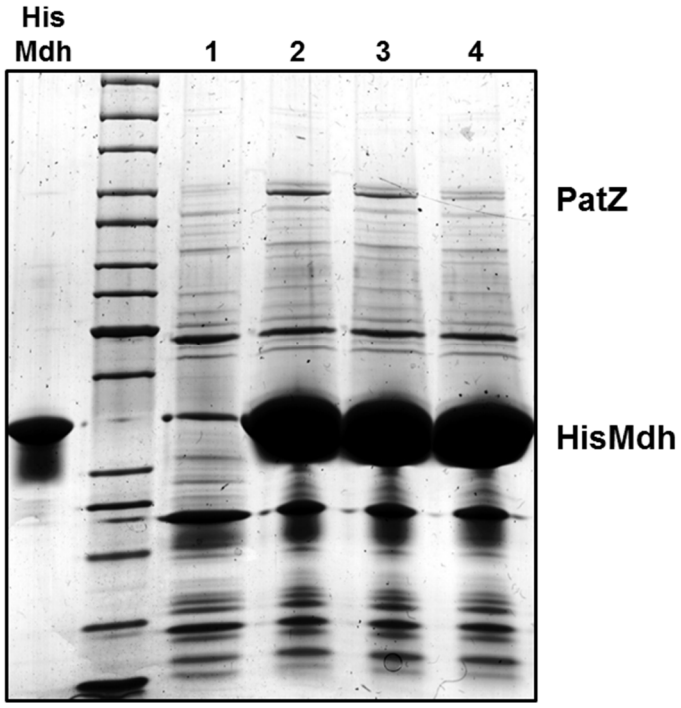

Figure III-3. Malate dehydrogenase interacts with PatZ depending on NADH.

Ligand fishing experiment was performed to confirm the interaction between Mdh and PatZ. Crude extract prepared from *E. coli* MG1655 cells was mixed with buffer A (lane 1) or 150 μg of Purified HisMdh (lanes 2-4). The extracts containing HisMdh was supplemented with either 2 mM NAD^+ (lane 3) or 2 mM NADH (lane 4) to assess the effect of these cofactors on the interaction. Each mixture was subjected to TALON metal affinity chromatography, followed by staining with Coomassie brilliant blue R.

4.2 Malate dehydrogenase modulates the acetyltransferase activity of PatZ

To examine whether the interaction between malate dehydrogenase and PatZ affect the enzymatic function of each enzyme, I purified the two proteins and performed in vitro activity assay in the presence of the other enzyme. As the copy number of Mdh protein was reported to be 30,000~ 80,000, while that of PatZ to be less than 100 in *E. coli*, PatZ protein was predicted to modulate the activity of Mdh through acetylation, not merely by simple binding (Schmidt et al., 2016). Nevertheless, the bidirectional activities of Malate dehydrogenase were not changed even after the incubation with PatZ or with both PatZ and acetyl-coA which was necessary for acetylation (Figure III-4). It has been reported that some lysine residues of malate dehydrogenase are acetylated when cells are grown on glucose, yet these residues are non-enzymatically acetylated by acetyl phosphate, not by PatZ (Schilling et al., 2015; Venkat et al., 2017). Therefore, I concluded that PatZ is incapable of regulating the activity of malate dehydrogenase.

Then, I tested if malate dehydrogenase could modulate the acetyltransferase activity of PatZ in reverse (Figure III-5). Because acetyl-coA synthetase (Acs) protein was reported to be acetylated by PatZ (de Diego Puente et al., 2015), I used purified strep-tagged Acs (StrepAcs) as a substrate of PatZ-mediated acetylation. The purified Acs proteins were mixed with PatZ and acetyl-coA in the presence and absence of Mdh. After 1h incubation at 37 ˚C, samples were subjected to SDS/PAGE, followed by immune-detection using anti-acetyllysine monoclonal antibody. While the acetylated Acs band was enriched in the presence of both PatZ and AcCoA, the band intensity was decreased in the column of samples with Mdh, suggesting that Malate dehydrogenase inhibits the acetyltransferase activity of PatZ. In the ligand-fishing data, I found that the binding of NADH to Mdh could block the

interaction between the two enzymes. Hence, to evaluate the effect of NADH on the inhibitory function of Mdh, Mdh was mixed with PatZ, after incubated with either 2 mM NAD^+ or 2 mM NADH and the acetylation assay was performed. While both Mdh and Mdh incubated with NAD^+ could inhibit the acetylation of Acs by PatZ, Acs in the set with NADH could be acetylated as in the set without Mdh. Thus, I concluded that Mdh inhibits the acetyltransferase activity of PatZ in the NADH-dependent manner.

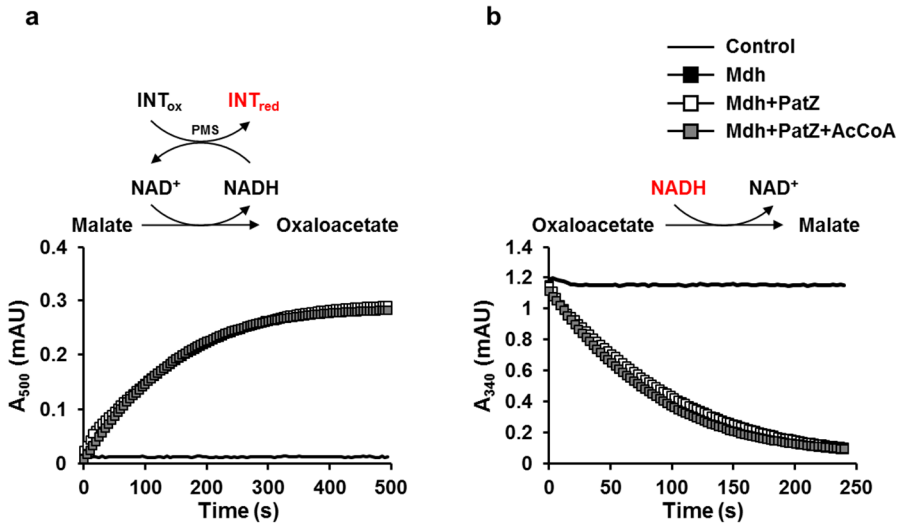

Figure III-4. PatZ is not involved in the regulation of the activity of Malate dehydrogenase

The bidirectional activity of malate dehydrogenase was assessed in the presence of either PatZ or both PatZ and AcCoA as indicated. **a,** The malate oxidation by malate dehydrogenase was quantified using the PMS-INT colorimetric assay, in which the production of NADH is coupled to reduction of INT which can be determined at 500 nm. **b,** The reaction converting oxaloacetate to malate was quantified by measuring the decrease of NADH at 340 nm.

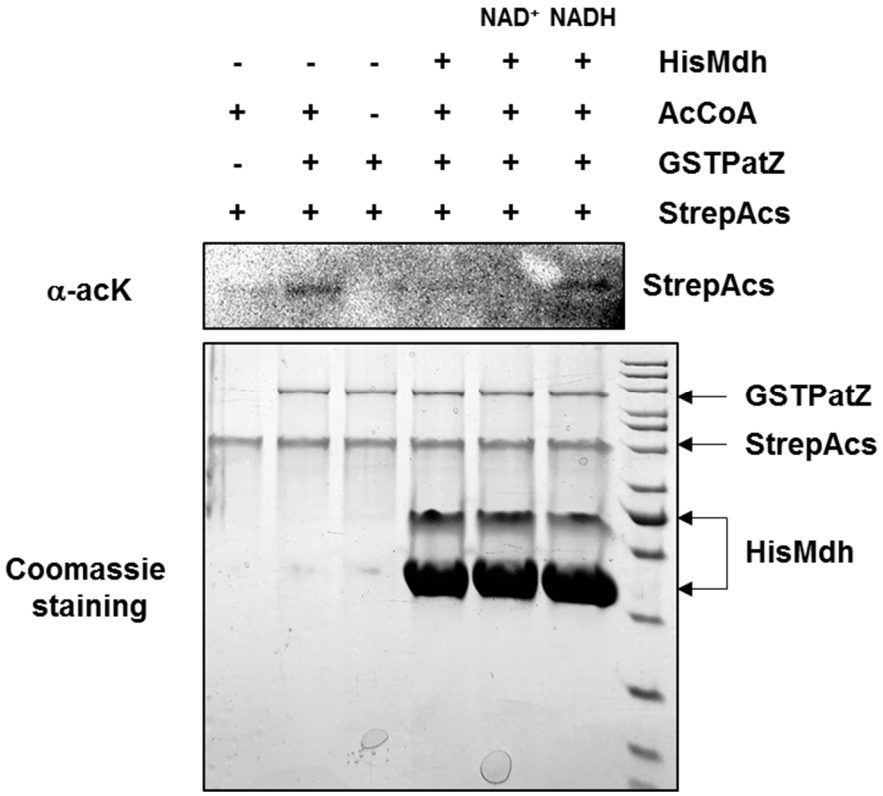

Figure III-5. Malate dehydrogenase inhibits the acetyltransferase activity of PatZ

The acetyltransferase activity of PatZ was determined by the amount of acetylated strep-tagged acetyl-coA synthetase (StrepAcs). PatZ was incubated with StrepAcs and 1 mM of acetyl coA at 37 ˚C for 1 h and its acetyltransferase activity was measured in the presence of different combinations of 20 μM HisMdh, 2 mM NAD^+, and 2 mM NADH. After incubation, each mixture was subjected to SDS/PAGE, followed by immunodetection using anti-acetyllysine antibody or Coomassie brilliant blue R for loading control.

4.3 PatZ regulates the metabolic fluxes enhancing the gluconeogenic growth of the cell on TCA intermediates.

PatZ is one of the GNAT-family lysine acetyltransferases and known to be involved in the regulation of many biological processes such as metabolism (Christensen et al., 2018), chemotaxis, RNA degradation, and protein stability (Christensen et al., 2019; Pisithkul et al., 2015). In *Gamma-proteobacteria*, it has been reported that the acetylated proteins by PatZ are largely involved in the carbon metabolism (Pisithkul et al., 2015; Schilling et al., 2015). In *Salmonella enterica*, PatZ acetylates the central metabolic enzymes enhancing the flux of glycolysis over gluconeogenesis and controls metabolism at the branching point between the TCA cycle and glyoxylate shunt pathway (Wang et al., 2010). In *E. coli* K strains, metabolic regulation performed by PatZ has been only studied in the aspect of acetate reconsumption (Castano-Cerezo et al., 2014).

To determine how PatZ regulates the central carbon metabolism, I compared the growth patterns of wild-type *E. coli* MG1655 cells and its *patZ*-deletion derivatives in the M9 minimal medium supplemented with a sole carbon source of either glycolytic sugars, such as glucose, galactose, fructose, or gluconeogenic carbon sources including TCA intermediates (Figure III-6). While the two strains showed no growth differences in the medium supplemented with glucose or fructose, Δ*patZ* exhibited much slower growth in the medium supplemented with TCA intermediates, suggesting that PatZ facilitates the gluconeogenic growth of a cell on TCA intermediates.

Interestingly, when the wild-type and Δ*patZ* cells were grown on galactose, also metabolized through glycolysis like glucose, Δ*patZ* showed a rapid growth pattern than that of the wild-type cells. It has been reported that glucose metabolism in fast-growing *E. coli* was characterized as an overflow

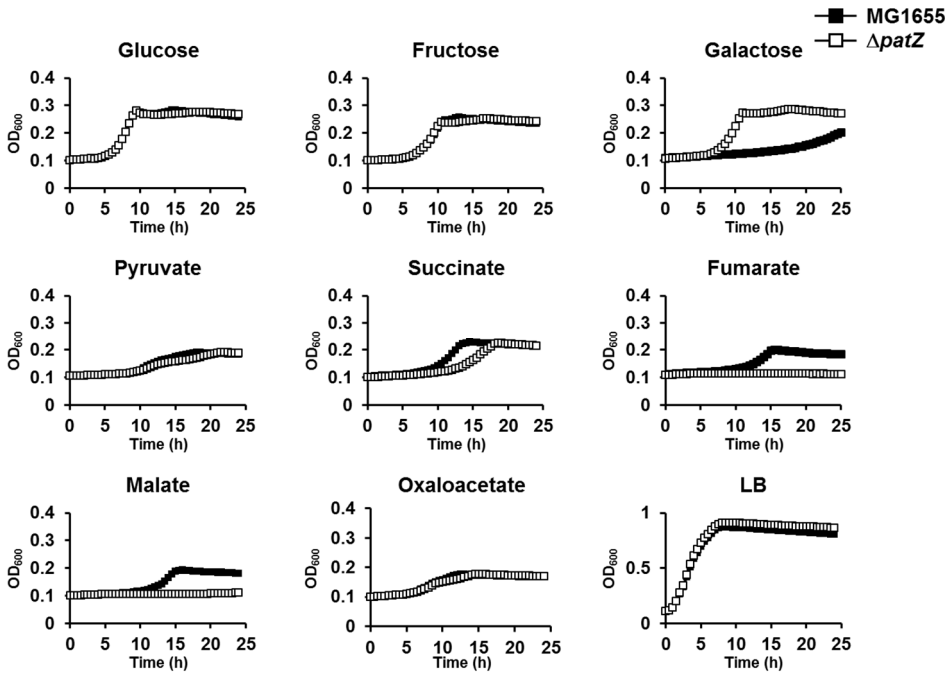

Figure III-6. An *E. coli* Δ*patZ* mutant shows retarded growth on gluconeogenic carbon sources.

Growth curves of the Δ*patZ* mutant was compared with the wild-type *E. coli* MG1655 strain in M9 minimal medium supplemented with the indicated carbon sources. The bacterial growth was recorded in triplicates by measuring the absorbance at 600 nm at 37 ˚C in a multimode microplate reader (TECAN). Growth curves in LB medium was used as control.

metabolism where most carbon flux is incorporated to the mixed acid fermentation producing acetate, lactate, succinate and formate (Wolfe, 2005). Conversely, when galactose was imported into the cell, it metabolized through glycolysis and the intact respiratory TCA cycle, without the production of acetic acid (Haverkorn van Rijsewijk et al., 2011). Thus I assumed that the observed effect of PatZ in the medium supplemented with galactose might be the result of different direction of metabolic flux, especially due to the reaction catalyzed by Mdh that proceeds to the opposite direction under the two conditions.

To verify this assumption, I compared the growth curves of the *ptsG*-deleted MG1655 mutant (Δ*ptsG*) and its isogenic *patZ* mutant (Δ*ptsG patZ*) in M9 minimal medium supplemented with glucose (Figure III-7). In *E. coli*, glucose is mainly transported through the phosphoenolpyruvate (PEP):carbohydrate phosphotransferase system (PTS) system with the concomitant phosphorylation. Therefore, the deletion of *ptsG* gene encoding the membrane-spanning glucose permease is expected to reduce the uptake rate of glucose and result in metabolic shift from mixed acid fermentation to respiratory TCA cycle (Postma et al., 1993). As expected, the additional deletion of *patZ* gene in Δ*ptsG* mutant increased the growth rate on glucose, implying that the inhibitory effect of PatZ on glycolytic growth was released. Thus I concluded that when malate dehydrogenase catalyzes malate oxidation, malate dehydrogenase loses its inhibitory effect on PatZ and PatZ modulates the metabolism.

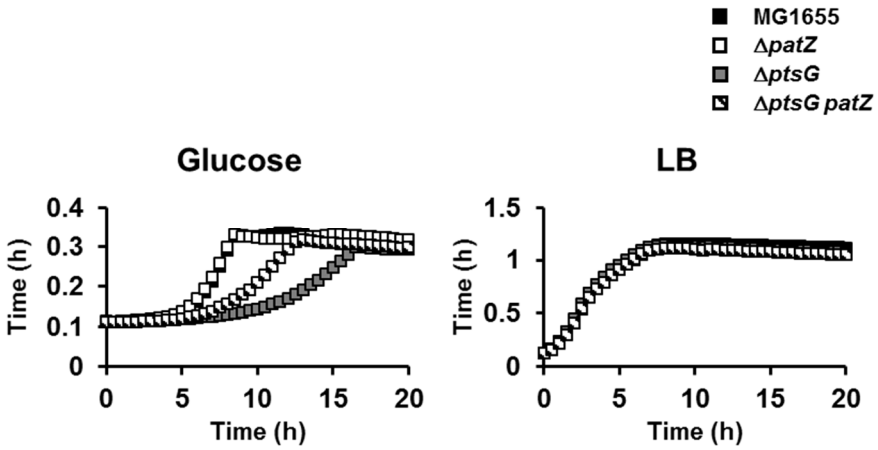

Figure III-7. PatZ regulates the metabolic flux in the slow-growing cells in glucose medium.

Growth curves of the indicated mutants were compared with the wild-type *E. coli* MG1655 strain in M9 minimal medium supplemented with 0.1% glucose. The bacterial growth was recorded in triplicates by measuring the absorbance at 600 nm at 37 ˚C in a multimode microplate reader (TECAN). Growth curves in LB medium was used as control.

4.4 PatZ regulates the metabolic fluxes by controlling the synthesis of α-ketoglutarate

Next, to investigate the molecular mechanism of these growth differences, I quantitatively analyzed metabolites extracted from wild-type MG1655 and Δ*patZ* cells grown in the M9 minimal medium supplemented with galactose using LC-MS/MS. The level of α-ketoglutarate dramatically decreases in the Δ*patZ* cells, inferring that the synthesis of α-ketoglutarate or the related metabolic pathway limits the growth rate in the wild-type cells. Previous studies in *salmonella enterica* revealed that PatZ modulates metabolism at the branch between oxidative TCA and glyoxylate bypass. It has been suggested that PatZ acetylates both isocitrate lyase (AceA) and isocitrate dehydrogenase kinase (AceK), so that it could regulate the proportion of ICDH activity over AceA activity (Wang et al., 2010). Thus, I assumed that the glyoxylate shunt might be stimulated in Δ*patZ* cells. I could also find that the AcCoA level in the wild-type cells is slightly higher than that of the mutant cells, supporting the previous hypothesis.

Collectively, I concluded that the acetyltransferase activity of PatZ is inhibited by malate dehydrogenase in the fast-growing cells in glucose medium. However, in the presence of carbohydrate which is slowly transported and metabolized through the intact oxidative TCA cycle and respiration, the PatZ activity is released from the inhibition by malate dehydrogenase and represses the glyoxylate shunt, enabling bacteria to generate NADH for energy biogenesis.

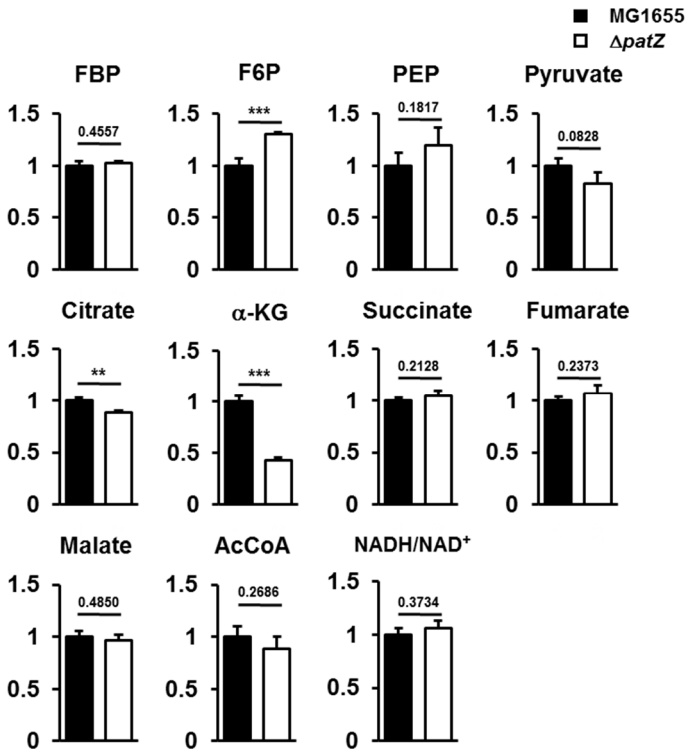

Figure III-8. Growth differences between wild-type MG1655 and Δ*patZ* is related to the synthesis of α-ketoglutarate.

The intracellular concentrations of metabolites were measured in wild-type MG1655 and a Δ*patZ* strain grown in M9 minimal medium supplemented with 0.1% galactose. The concentration of each metabolite extracted from the *E. coli* cells was determined using LC-MS/MS. Statistical significance was assessed using Student's *t*-test (*p values* greater than 0.05 were presented, ***p* value <0.01, ****p* value <0.005). Shown are the means and SD (n=3, independent measurements).

5. Discussion

Adaptation to metabolic fluctuations is crucial for the survival and propagation of the cell. The canonical model for these responses is through the transmembrane or intracellular receptors which sense the extracellular cues and transduce this information to the cognate signal transduction system (Stock et al., 2000; Ulrich et al., 2005). However, *E. coli* can grow on up to 180 carbon sources according to the computational prediction using its genomic sequence (Orth et al., 2011) and the expression of each receptor to each one of 180 carbohydrates can be overwhelming to cells. Recently, more efficient way has been reported by which bacteria senses and transduces these metabolic signals (Litsios et al., 2018). By sensing the intracellular flux and the integrated information of multiple nutrional inputs, bacteria can economically react to any metabolic shift of the cells.

In this study, I suggested a novel flux-dependent signal transduction module that consists of flux-signaling metabolite NADH and its effector enzyme malate dehydrogenase. Metabolomics studies in *E. coli* have reported that the intracellular concentration of NADH exceeds the K_m values of the NADH-utilizing enzymes, including malate dehydrogenase, depending on growth conditions, while NAD^+ consistently exists in more than ten-fold higher concentration than K_m values of the enzymes (Bennett et al., 2009). Also, under oxidative stress or carbon overflow metabolism, the reductive TCA cycle is employed for NADH oxidation to prevent its accumulation (Chakraborty et al., 2020; Shimizu and Matsuoka, 2019), indicating that malate dehydrogenase deliberately senses the shift in the concentration of NADH in a cell.

Here, I showed that malate dehydrogenase modulates the acetyltransferase activity of PatZ in the NADH-dependent manner. Previous studies have shown that post-translational modifications (PTMs) on various enzymes

affect their activities or stabilities, and regulate the related phenotypes without additional expression or degradation of proteins (Cain et al., 2014). In particular, the regulation of metabolism by PTMs is economical, as metabolic fluxes consist of enormous number of enzymes. Among PTM, acetylation is thought to be deeply involved in the regulation of metabolic enzymes, because two distinct acetylation mechanisms, the non-enzymatic acetylation by acetyl-phosphate (AcP) and the enzymatic acetylation by acetyltransferase, utilize the metabolic intermediates as an acetyl donor (Pisithkul et al., 2015; Weinert et al., 2013). However, the only regulatory mechanism of the acetyltransferase is the regulation of its expression by the cAMP-CRP complex (Castano-Cerezo et al., 2011). My model suggest a mechanism how the acetyltransferase responds to the metabolic perturbations, leading to an immediate and efficient regulation of metabolic enzymes and thus metabolic fluxes by acetylation.

6. References

Adler, J., Hazelbauer, G.L., and Dahl, M.M. (1973). Chemotaxis toward sugars in *Escherichia coli*. J Bacteriol *115*, 824-847.

Adler, J., and Templeton, B. (1967). The effect of environmental conditions on the motility of *Escherichia coli*. J Gen Microbiol *46*, 175-184.

Bang, I., Kim, H.R., Beaven, A.H., Kim, J., Ko, S.B., Lee, G.R., Kan, W., Lee, H., Im, W., Seok, C.*, et al.* (2018). Biophysical and functional characterization of Norrin signaling through Frizzled4. Proc Natl Acad Sci U S A *115*, 8787-8792.

Barabote, R.D., and Saier, M.H., Jr. (2005). Comparative genomic analyses of the bacterial phosphotransferase system. Microbiol Mol Biol Rev *69*, 608-634.

Basan, M., Hui, S., Okano, H., Zhang, Z., Shen, Y., Williamson, J.R., and Hwa, T. (2015). Overflow metabolism in *Escherichia coli* results from efficient proteome allocation. Nature *528*, 99-104.

Bennett, B.D., Kimball, E.H., Gao, M., Osterhout, R., Van Dien, S.J., and Rabinowitz, J.D. (2009). Absolute metabolite concentrations and implied enzyme active site occupancy in *Escherichia coli*. Nat Chem Biol *5*, 593-599.

Bettenbrock, K., Sauter, T., Jahreis, K., Kremling, A., Lengeler, J.W., and Gilles, E.D. (2007). Correlation between growth rates, EIIACrr phosphorylation, and intracellular cyclic AMP levels in *Escherichia coli* K-12. J Bacteriol *189*, 6891-6900.

Beyhan, S., Bilecen, K., Salama, S.R., Casper-Lindley, C., and Yildiz, F.H. (2007). Regulation of rugosity and biofilm formation in *Vibrio cholerae*: comparison of VpsT and VpsR regulons and epistasis analysis of *vpsT*, *vpsR*, and *hapR*. J Bacteriol *189*, 388-402.

Blokesch, M. (2012). Chitin colonization, chitin degradation and chitin-

induced natural competence of *Vibrio cholerae* are subject to catabolite repression. Environ Microbiol *14*, 1898-1912.

Blow, N.S., Salomon, R.N., Garrity, K., Reveillaud, I., Kopin, A., Jackson, F.R., and Watnick, P.I. (2005). *Vibrio cholerae* infection of *Drosophila melanogaster* mimics the human disease cholera. PLoS Pathog *1*, e8.

Butler, S.M., and Camilli, A. (2005). Going against the grain: chemotaxis and infection in *Vibrio cholerae*. Nat Rev Microbiol *3*, 611-620.

Cain, J.A., Solis, N., and Cordwell, S.J. (2014). Beyond gene expression: the impact of protein post-translational modifications in bacteria. J Proteomics *97*, 265-286.

Castano-Cerezo, S., Bernal, V., Blanco-Catala, J., Iborra, J.L., and Canovas, M. (2011). cAMP-CRP co-ordinates the expression of the protein acetylation pathway with central metabolism in *Escherichia coli*. Mol Microbiol *82*, 1110-1128.

Castano-Cerezo, S., Bernal, V., Post, H., Fuhrer, T., Cappadona, S., Sanchez-Diaz, N.C., Sauer, U., Heck, A.J., Altelaar, A.F., and Canovas, M. (2014). Protein acetylation affects acetate metabolism, motility and acid stress response in *Escherichia coli*. Mol Syst Biol *10*, 762.

Chakraborty, S., Liu, L., Fitzsimmons, L., Porwollik, S., Kim, J.S., Desai, P., McClelland, M., and Vazquez-Torres, A. (2020). Glycolytic reprograming in *Salmonella* counters NOX2-mediated dissipation of DpH. Nat Commun *11*, 1783.

Christensen, D.G., Meyer, J.G., Baumgartner, J.T., D'Souza, A.K., Nelson, W.C., Payne, S.H., Kuhn, M.L., Schilling, B., and Wolfe, A.J. (2018). Identification of Novel Protein Lysine Acetyltransferases in *Escherichia coli*. mBio *9*.

Christensen, D.G., Xie, X., Basisty, N., Byrnes, J., McSweeney, S., Schilling, Mechanism for Bacteria to Dynamically Regulate Metabolic Functions. Front Microbiol *10*, 1604.

Chua, S.L., Liu, Y., Yam, J.K., Chen, Y., Vejborg, R.M., Tan, B.G., Kjelleberg, S., Tolker-Nielsen, T., Givskov, M., and Yang, L. (2014). Dispersed cells represent a distinct stage in the transition from bacterial biofilm to planktonic lifestyles. Nat Commun *5*, 4462.

Contesse, G., Crepin, M., and Gros, F. (1969). [Transcription of the lactose operon in *Escherichia coli* mutants]. C R Acad Hebd Seances Acad Sci D *268*, 2301-2304.

Correa, N.E., Peng, F., and Klose, K.E. (2005). Roles of the regulatory proteins FlhF and FlhG in the *Vibrio cholerae* flagellar transcription hierarchy. J Bacteriol *187*, 6324-6332.

Cotter, P.A., and Stibitz, S. (2007). c-di-GMP-mediated regulation of virulence and biofilm formation. Curr Opin Microbiol *10*, 17-23.

de Diego Puente, T., Gallego-Jara, J., Castano-Cerezo, S., Bernal Sanchez, V., Fernandez Espin, V., Garcia de la Torre, J., Manjon Rubio, A., and Canovas Diaz, M. (2015). The Protein Acetyltransferase PatZ from *Escherichia coli* Is Regulated by Autoacetylation-induced Oligomerization. J Biol Chem *290*, 23077-23093.

Deutscher, J., Ake, F.M., Derkaoui, M., Zebre, A.C., Cao, T.N., Bouraoui, H., Kentache, T., Mokhtari, A., Milohanic, E., and Joyet, P. (2014a). The bacterial phosphoenolpyruvate:carbohydrate phosphotransferase system: regulation by protein phosphorylation and phosphorylation-dependent protein-protein interactions. Microbiol Mol Biol Rev *78*, 231-256.

Deutscher, J., Aké, F.M., Derkaoui, M., Zébré, A.C., Cao, T.N., Bouraoui, H., Kentache, T., Mokhtari, A., Milohanic, E., and Joyet, P. (2014b). The bacterial phosphoenolpyruvate:carbohydrate phosphotransferase system: regulation by protein phosphorylation and phosphorylation-dependent protein-protein interactions. Microbiol Mol Biol Rev *78*, 231-256.

Deutscher, J., Francke, C., and Postma, P.W. (2006). How phosphotransferase system-related protein phosphorylation regulates carbohydrate metabolism

in bacteria. Microbiol Mol Biol Rev *70*, 939-1031.

Dobrogosz, W.J., and Hamilton, P.B. (1971). The role of cyclic AMP in chemotaxis in *Escherichia coli*. Biochem Biophys Res Commun *42*, 202-207.

Farewell, A., Kvint, K., and Nystrom, T. (1998). Negative regulation by RpoS: a case of sigma factor competition. Mol Microbiol *29*, 1039-1051.

Flemming, H.C., and Wingender, J. (2010). The biofilm matrix. Nat Rev Microbiol *8*, 623-633.

Fong, J.C., and Yildiz, F.H. (2008). Interplay between cyclic AMP-cyclic AMP receptor protein and cyclic di-GMP signaling in *Vibrio cholerae* biofilm formation. J Bacteriol *190*, 6646-6659.

Gaal, T., Ross, W., Estrem, S.T., Nguyen, L.H., Burgess, R.R., and Gourse, R.L. (2001). Promoter recognition and discrimination by EsigmaS RNA polymerase. Mol Microbiol *42*, 939-954.

Galperin, M.Y., Nikolskaya, A.N., and Koonin, E.V. (2001). Novel domains of the prokaryotic two-component signal transduction systems. FEMS Microbiol Lett *203*, 11-21.

Gerosa, L., and Sauer, U. (2011). Regulation and control of metabolic fluxes in microbes. Curr Opin Biotechnol *22*, 566-575.

Gjermansen, M., Ragas, P., Sternberg, C., Molin, S., and Tolker-Nielsen, T. (2005). Characterization of starvation-induced dispersion in *Pseudomonas putida* biofilms. Environ Microbiol *7*, 894-906.

Gorke, B., and Stulke, J. (2008). Carbon catabolite repression in bacteria: many ways to make the most out of nutrients. Nat Rev Microbiol *6*, 613-624.

Ha, E.M., Lee, K.A., Seo, Y.Y., Kim, S.H., Lim, J.H., Oh, B.H., Kim, J., and Lee, W.J. (2009). Coordination of multiple dual oxidase-regulatory pathways in responses to commensal and infectious microbes in *drosophila* gut. Nat Immunol *10*, 949-957.

Hansen, M.T., Pato, M.L., Molin, S., Fill, N.P., and von Meyenburg, K. (1975). Simple downshift and resulting lack of correlation between ppGpp pool size and ribonucleic acid accumulation. J Bacteriol *122*, 585-591.

Haverkorn van Rijsewijk, B.R., Nanchen, A., Nallet, S., Kleijn, R.J., and Sauer, U. (2011). Large-scale ^{13}C-flux analysis reveals distinct transcriptional control of respiratory and fermentative metabolism in *Escherichia coli*. Mol Syst Biol *7*, 477.

Hayes, C.A., Dalia, T.N., and Dalia, A.B. (2017). Systematic genetic dissection of PTS in *Vibrio cholerae* uncovers a novel glucose transporter and a limited role for PTS during infection of a mammalian host. Mol Microbiol *104*, 568-579.

Hengge, R. (2009). Principles of c-di-GMP signalling in bacteria. Nat Rev Microbiol *7*, 263-273.

Hermsen, R., Okano, H., You, C., Werner, N., and Hwa, T. (2015). A growth-rate composition formula for the growth of E.coli on co-utilized carbon substrates. Mol Syst Biol *11*, 801.

Hogema, B.M., Arents, J.C., Bader, R., Eijkemans, K., Yoshida, H., Takahashi, H., Aiba, H., and Postma, P.W. (1998). Inducer exclusion in *Escherichia coli* by non-PTS substrates: the role of the PEP to pyruvate ratio in determining the phosphorylation state of enzyme IIA^{Glc}. Mol Microbiol *30*, 487-498.

Houot, L., Chang, S., Absalon, C., and Watnick, P.I. (2010a). *Vibrio cholerae* phosphoenolpyruvate phosphotransferase system control of carbohydrate transport, biofilm formation, and colonization of the germfree mouse intestine. Infect Immun *78*, 1482-1494.

Houot, L., Chang, S., Pickering, B.S., Absalon, C., and Watnick, P.I. (2010b). The phosphoenolpyruvate phosphotransferase system regulates *Vibrio cholerae* biofilm formation through multiple independent pathways. J Bacteriol *192*, 3055-3067.

Houot, L., and Watnick, P.I. (2008). A novel role for enzyme I of the *Vibrio cholerae* phosphoenolpyruvate phosphotransferase system in regulation of growth in a biofilm. J Bacteriol *190*, 311-320.

Hui, S., Silverman, J.M., Chen, S.S., Erickson, D.W., Basan, M., Wang, J., Hwa, T., and Williamson, J.R. (2015). Quantitative proteomic analysis reveals a simple strategy of global resource allocation in bacteria. Mol Syst Biol *11*, 784.

Jones, M.K., Warner, E.B., and Oliver, J.D. (2008). *csrA* inhibits the formation of biofilms by *Vibrio vulnificus*. Appl Environ Microbiol *74*, 7064-7066.

Kamareddine, L., Wong, A.C.N., Vanhove, A.S., Hang, S., Purdy, A.E., Kierek-Pearson, K., Asara, J.M., Ali, A., Morris, J.G., Jr., and Watnick, P.I. (2018). Activation of *Vibrio cholerae* quorum sensing promotes survival of an arthropod host. Nat Microbiol *3*, 243-252.

Kaplan, J.B. (2010). Biofilm dispersal: mechanisms, clinical implications, and potential therapeutic uses. J Dent Res *89*, 205-218.

Karatan, E., and Watnick, P. (2009). Signals, regulatory networks, and materials that build and break bacterial biofilms. Microbiol Mol Biol Rev *73*, 310-347.

Kierek, K., and Watnick, P.I. (2003). Environmental determinants of *Vibrio cholerae* biofilm development. Appl Environ Microbiol *69*, 5079-5088.

Kim, H.M., Park, Y.H., Yoon, C.K., and Seok, Y.J. (2015). Histidine phosphocarrier protein regulates pyruvate kinase A activity in response to glucose in *Vibrio vulnificus*. Mol Microbiol *96*, 293-305.

Kim, Y.J., Ryu, Y., Koo, B.M., Lee, N.Y., Chun, S.J., Park, S.J., Lee, K.H., and Seok, Y.J. (2010). A mammalian insulysin homolog is regulated by enzyme IIA^{Glc} of the glucose transport system in *Vibrio vulnificus*. FEBS Lett *584*, 4537-4544.

Kochanowski, K., Volkmer, B., Gerosa, L., Haverkorn van Rijsewijk, B.R.,

Schmidt, A., and Heinemann, M. (2013). Functioning of a metabolic flux sensor in *Escherichia coli*. Proc Natl Acad Sci U S A *110*, 1130-1135.

Koo, B.M., Yoon, M.J., Lee, C.R., Nam, T.W., Choe, Y.J., Jaffe, H., Peterkofsky, A., and Seok, Y.J. (2004). A novel fermentation/respiration switch protein regulated by enzyme IIA^{Glc} in *Escherichia coli*. J Biol Chem *279*, 31613-31621.

Kotte, O., Zaugg, J.B., and Heinemann, M. (2010). Bacterial adaptation through distributed sensing of metabolic fluxes. Mol Syst Biol *6*, 355.

Kundig, W., Ghosh, S., and Roseman, S. (1964). Phosphate Bound to Histidine in a Protein as an Intermediate in a Novel Phospho-Transferase System. Proc Natl Acad Sci U S A *52*, 1067-1074.

Lazzarini, R.A., Cashel, M., and Gallant, J. (1971). On the regulation of guanosine tetraphosphate levels in stringent and relaxed strains of *Escherichia coli*. J Biol Chem *246*, 4381-4385.

Lee, C.R., Park, Y.H., Min, H., Kim, Y.R., and Seok, Y.J. (2019). Determination of protein phosphorylation by polyacrylamide gel electrophoresis. J Microbiol *57*, 93-100.

Lee, J.W., Park, Y.H., and Seok, Y.J. (2018). Rsd balances (p)ppGpp level by stimulating the hydrolase activity of SpoT during carbon source downshift in *Escherichia coli*. Proc Natl Acad Sci U S A *115*, E6845-E6854.

Lee, K.J., Kim, J.A., Hwang, W., Park, S.J., and Lee, K.H. (2013). Role of capsular polysaccharide (CPS) in biofilm formation and regulation of CPS production by quorum-sensing in *Vibrio vulnificus*. Mol Microbiol *90*, 841-857.

Lendenmann, U., Snozzi, M., and Egli, T. (1996). Kinetics of the simultaneous utilization of sugar mixtures by *Escherichia coli* in continuous culture. Appl Environ Microbiol *62*, 1493-1499.

Leng, Y., Vakulskas, C.A., Zere, T.R., Pickering, B.S., Watnick, P.I., Babitzke, P., and Romeo, T. (2016). Regulation of CsrB/C sRNA decay by $EIIA^{Glc}$ of

the phosphoenolpyruvate: carbohydrate phosphotransferase system. Mol Microbiol *99*, 627-639.

Li, X., Gianoulis, T.A., Yip, K.Y., Gerstein, M., and Snyder, M. (2010). Extensive in vivo metabolite-protein interactions revealed by large-scale systematic analyses. Cell *143*, 639-650.

Liang, W., Pascual-Montano, A., Silva, A.J., and Benitez, J.A. (2007). The cyclic AMP receptor protein modulates quorum sensing, motility and multiple genes that affect intestinal colonization in *Vibrio cholerae*. Microbiology *153*, 2964-2975.

Link, H., Kochanowski, K., and Sauer, U. (2013). Systematic identification of allosteric protein-metabolite interactions that control enzyme activity in vivo. Nat Biotechnol *31*, 357-361.

Litsios, A., Ortega, A.D., Wit, E.C., and Heinemann, M. (2018). Metabolic-flux dependent regulation of microbial physiology. Curr Opin Microbiol *42*, 71-78.

Loomis, W.F., Jr., and Magasanik, B. (1967). Glucose-lactose diauxie in *Escherichia coli*. J Bacteriol *93*, 1397-1401.

Mistry, R., Kounatidis, I., and Ligoxygakis, P. (2016). Exploring interactions between pathogens and the *Drosophila* gut. Dev Comp Immunol *64*, 3-10.

Moisi, M., Jenul, C., Butler, S.M., New, A., Tutz, S., Reidl, J., Klose, K.E., Camilli, A., and Schild, S. (2009). A novel regulatory protein involved in motility of *Vibrio cholerae*. J Bacteriol *191*, 7027-7038.

Nam, T.W., Park, Y.H., Jeong, H.J., Ryu, S., and Seok, Y.J. (2005). Glucose repression of the *Escherichia coli sdhCDAB* operon, revisited: regulation by the CRP·cAMP complex. Nucleic Acids Res *33*, 6712-6722.

O'Toole, G., Kaplan, H.B., and Kolter, R. (2000). Biofilm formation as microbial development. Annu Rev Microbiol *54*, 49-79.

Okano, H., Hermsen, R., Kochanowski, K., and Hwa, T. (2020). Regulation underlying hierarchical and simultaneous utilization of carbon substrates

by flux sensors in *Escherichia coli*. Nat Microbiol *5*, 206-215.

Orth, J.D., Conrad, T.M., Na, J., Lerman, J.A., Nam, H., Feist, A.M., and Palsson, B.O. (2011). A comprehensive genome-scale reconstruction of *Escherichia coli* metabolism. Mol Syst Biol *7*, 535.

Park, S., Park, Y.H., Lee, C.R., Kim, Y.R., and Seok, Y.J. (2016). Glucose induces delocalization of a flagellar biosynthesis protein from the flagellated pole. Mol Microbiol *101*, 795-808.

Park, S., Yoon, J., Lee, C.R., Lee, J.Y., Kim, Y.R., Jang, K.S., Lee, K.H., and Seok, Y.J. (2019). Polar landmark protein HubP recruits flagella assembly protein FapA under glucose limitation in *Vibrio vulnificus*. Mol Microbiol *112*, 266-279.

Park, Y.H., Lee, B.R., Seok, Y.J., and Peterkofsky, A. (2006). In vitro reconstitution of catabolite repression in *Escherichia coli*. J Biol Chem *281*, 6448-6454.

Park, Y.H., Lee, C.R., Choe, M., and Seok, Y.J. (2013a). HPr antagonizes the anti-σ^{70} activity of Rsd in *Escherichia coli*. Proc Natl Acad Sci U S A *110*, 21142-21147.

Pickering, B.S., Lopilato, J.E., Smith, D.R., and Watnick, P.I. (2014). The transcription factor Mlc promotes *Vibrio cholerae* biofilm formation through repression of phosphotransferase system components. J Bacteriol *196*, 2423-2430.

Pickering, B.S., Smith, D.R., and Watnick, P.I. (2012). Glucose-specific enzyme IIA has unique binding partners in the *vibrio cholerae* biofilm. mBio *3*, e00228-00212.

Piper, S.E., Mitchell, J.E., Lee, D.J., and Busby, S.J. (2009). A global view of *Escherichia coli* Rsd protein and its interactions. Mol Biosyst *5*, 1943-1947.

Pisithkul, T., Patel, N.M., and Amador-Noguez, D. (2015). Post-translational Microbiol *24*, 29-37.

Postma, P.W., Lengeler, J.W., and Jacobson, G.R. (1993).

Phosphoenolpyruvate:carbohydrate phosphotransferase systems of bacteria. Microbiol Rev *57*, 543-594.

Purdy, A.E., and Watnick, P.I. (2011). Spatially selective colonization of the arthropod intestine through activation of *Vibrio cholerae* biofilm formation. Proc Natl Acad Sci U S A *108*, 19737-19742.

Ramseier, T.M., Bledig, S., Michotey, V., Feghali, R., and Saier, M.H., Jr. (1995). The global regulatory protein FruR modulates the direction of carbon flow in *Escherichia coli*. Mol Microbiol *16*, 1157-1169.

Ramseier, T.M., Negre, D., Cortay, J.C., Scarabel, M., Cozzone, A.J., and Saier, M.H., Jr. (1993). In vitro binding of the pleiotropic transcriptional regulatory protein, FruR, to the *fru*, *pps*, *ace*, *pts* and *icd* operons of *Escherichia coli* and *Salmonella typhimurium*. J Mol Biol *234*, 28-44.

Roelofs, K.G., Jones, C.J., Helman, S.R., Shang, X., Orr, M.W., Goodson, J.R., Galperin, M.Y., Yildiz, F.H., and Lee, V.T. (2015). Systematic Identification of Cyclic-di-GMP Binding Proteins in *Vibrio cholerae* Reveals a Novel Class of Cyclic-di-GMP-Binding ATPases Associated with Type II Secretion Systems. PLoS Pathog *11*, e1005232.

Ryjenkov, D.A., Simm, R., Römling, U., and Gomelsky, M. (2006). The PilZ domain is a receptor for the second messenger c-di-GMP: the PilZ domain protein YcgR controls motility in enterobacteria. J Biol Chem *281*, 30310-30314.

Ryu, S., Ramseier, T.M., Michotey, V., Saier, M.H., Jr., and Garges, S. (1995). Effect of the FruR regulator on transcription of the *pts* operon in *Escherichia coli*. J Biol Chem *270*, 2489-2496.

Sauer, K., Cullen, M.C., Rickard, A.H., Zeef, L.A., Davies, D.G., and Gilbert, P. (2004). Characterization of nutrient-induced dispersion in *Pseudomonas aeruginosa* PAO1 biofilm. J Bacteriol *186*, 7312-7326.

Schilling, B., Christensen, D., Davis, R., Sahu, A.K., Hu, L.I., Walker-Peddakotla, A., Sorensen, D.J., Zemaitaitis, B., Gibson, B.W., and Wolfe,

A.J. (2015). Protein acetylation dynamics in response to carbon overflow in *Escherichia coli*. Mol Microbiol *98*, 847-863.

Schleheck, D., Barraud, N., Klebensberger, J., Webb, J.S., McDougald, D., Rice, S.A., and Kjelleberg, S. (2009). *Pseudomonas aeruginosa* PAO1 preferentially grows as aggregates in liquid batch cultures and disperses upon starvation. PLoS One *4*, e5513.

Schmidt, A., Kochanowski, K., Vedelaar, S., Ahrné, E., Volkmer, B., Callipo, L., Knoops, K., Bauer, M., Aebersold, R., and Heinemann, M. (2016). The quantitative and condition-dependent *Escherichia coli* proteome. Nat Biotechnol *34*, 104-110.

Schmidt, A.J., Ryjenkov, D.A., and Gomelsky, M. (2005). The ubiquitous protein domain EAL is a cyclic diguanylate-specific phosphodiesterase: enzymatically active and inactive EAL domains. J Bacteriol *187*, 4774-4781.

Shimada, T., Yamamoto, K., and Ishihama, A. (2011). Novel members of the Cra regulon involved in carbon metabolism in *Escherichia coli*. J Bacteriol *193*, 649-659.

Shimizu, K., and Matsuoka, Y. (2019). Regulation of glycolytic flux and overflow metabolism depending on the source of energy generation for energy demand. Biotechnol Adv *37*, 284-305.

Silva, A.J., and Benitez, J.A. (2016). *Vibrio cholerae* Biofilms and Cholera Pathogenesis. PLoS Negl Trop Dis *10*, e0004330.

Singh, P.K., Bartalomej, S., Hartmann, R., Jeckel, H., Vidakovic, L., Nadell, C.D., and Drescher, K. (2017). *Vibrio cholerae* Combines Individual and Collective Sensing to Trigger Biofilm Dispersal. Curr Biol *27*, 3359-3366 e3357.

Starai, V.J., and Escalante-Semerena, J.C. (2004). Identification of the protein acetyltransferase (Pat) enzyme that acetylates acetyl-CoA synthetase in *Salmonella enterica*. J Mol Biol *340*, 1005-1012.

Stock, A.M., Robinson, V.L., and Goudreau, P.N. (2000). Two-component signal transduction. Annu Rev Biochem *69*, 183-215.

Stutzmann, S., and Blokesch, M. (2016). Circulation of a Quorum-Sensing-Impaired Variant of *Vibrio cholerae* Strain C6706 Masks Important Phenotypes. mSphere *1*.

Tchieu, J.H., Norris, V., Edwards, J.S., and Saier, M.H., Jr. (2001). The complete phosphotransferase system in *Escherichia coli*. J Mol Microbiol Biotechnol *3*, 329-346.

Tchigvintsev, A., Xu, X., Singer, A., Chang, C., Brown, G., Proudfoot, M., Cui, H., Flick, R., Anderson, W.F., Joachimiak, A.*, et al.* (2010). Structural insight into the mechanism of c-di-GMP hydrolysis by EAL domain phosphodiesterases. J Mol Biol *402*, 524-538.

Tischler, A.D., and Camilli, A. (2004). Cyclic diguanylate (c-di-GMP) regulates *Vibrio cholerae* biofilm formation. Mol Microbiol *53*, 857-869.

Ulrich, L.E., Koonin, E.V., and Zhulin, I.B. (2005). One-component systems dominate signal transduction in prokaryotes. Trends Microbiol *13*, 52-56.

Vakulskas, C.A., Potts, A.H., Babitzke, P., Ahmer, B.M., and Romeo, T. (2015). Regulation of bacterial virulence by Csr (Rsm) systems. Microbiol Mol Biol Rev *79*, 193-224.

Venkat, S., Gregory, C., Sturges, J., Gan, Q., and Fan, C. (2017). Studying the Lysine Acetylation of Malate Dehydrogenase. J Mol Biol *429*, 1396-1405.

Wang, Q., Zhang, Y., Yang, C., Xiong, H., Lin, Y., Yao, J., Li, H., Xie, L., Zhao, W., Yao, Y.*, et al.* (2010). Acetylation of metabolic enzymes coordinates carbon source utilization and metabolic flux. Science *327*, 1004-1007.

Warburg, O. (1956). On the origin of cancer cells. Science *123*, 309-314.

Watnick, P.I., and Kolter, R. (1999). Steps in the development of a *Vibrio cholerae* El Tor biofilm. Mol Microbiol *34*, 586-595.

Weinert, B.T., Iesmantavicius, V., Wagner, S.A., Scholz, C., Gummesson, B.,

Beli, P., Nystrom, T., and Choudhary, C. (2013). Acetyl-phosphate is a critical determinant of lysine acetylation in *E. coli*. Mol Cell *51*, 265-272.

Westblade, L.F., Ilag, L.L., Powell, A.K., Kolb, A., Robinson, C.V., and Busby, S.J. (2004). Studies of the *Escherichia coli* Rsd-sigma70 complex. J Mol Biol *335*, 685-692.

Wolfe, A.J. (2005). The acetate switch. Microbiol Mol Biol Rev *69*, 12-50.

You, C., Okano, H., Hui, S., Zhang, Z., Kim, M., Gunderson, C.W., Wang, Y.P., Lenz, P., Yan, D., and Hwa, T. (2013). Coordination of bacterial proteome with metabolism by cyclic AMP signalling. Nature *500*, 301-306.

Zhu, J., and Mekalanos, J.J. (2003). Quorum sensing-dependent biofilms enhance colonization in *Vibrio cholerae*. Dev Cell *5*, 647-656.

Zhu, J., Miller, M.B., Vance, R.E., Dziejman, M., Bassler, B.L., and Mekalanos, J.J. (2002). Quorum-sensing regulators control virulence gene expression in *Vibrio cholerae*. Proc Natl Acad Sci U S A *99*, 3129-3134.

Zwaig, N., and Lin, E.C. (1966). Feedback inhibition of glycerol kinase, a catabolic enzyme in *Escherichia coli*. Science *153*, 755-757.

국문 초록

박테리아에서 대사 신호에 따른 생물막 형성 및 대사 흐름 조절

박테리아는 수시로 변화하는 환경에 적응하기 위하여, 외부 자극을 빠르게 인지 및 대응할 수 있는 다양한 신호전달기전을 보유하고 있다. 특히, 영양분의 흡수 및 대사를 통한 생장, 분열이 최우선 과제인 미생물에게 대사 신호 (metabolic signal)는 매우 중요한 신호로 여겨지며, 이에 미생물은 대사 신호에 정교하게 반응할 수 있는 신호전달기전을 보유할 것으로 예상된다. 또한, 이러한 영양분의 역할 뿐 아니라, 대사 신호는 다양한 환경을 갖는 박테리아(특히 병원균)에서 특정 환경을 인지할 수 있도록 환경 특이적 인자로써 작용할 수 있기 때문에, 미생물에서의 대사 신호 의존적 생리조절연구는 큰 의미를 가질 수 있다.

여기서, 우리는 미생물의 두 가지 대사 신호 의존적 생리 조절 기작에 대해 연구하였다. 첫 번째로는 비브리오 콜레라균(*Vibrio cholerae*)에서 당 수송 인산전달계 (Phosphoenolpyruvate : carbohydrate phosphotransferase system, PTS)의 생물막 형성 조절 기전을 제시하였다. 당 수송 인산전달계 구성 단백질인 $EIIA^{Glc}$ 이 대표적 생물막 형성 조절자인 c-di-GMP 조절 효소와 상호작용하여, 이 효소의 활성을 조절한 다는 사실을 확인하였다. $EIIA^{Glc}$는 외부 당의 종류에 따라 다른 수준의 인산화 정도를 가

진다는 사실이 확인된 바 있었고, 우리는 이 인산화 상태에 의존적으로 비브리오 콜레라균의 생물막 형성을 조절한다는 사실은 확인하였다. 초파리 감염모델을 통하여 두 단백질의 상호작용이 병원균의 감염상황에서, 박테리아가 해당 환경에 머무를지, 떠날지를 판단하는 영양분 의존적 결정자로서 작용할 것이라는 것을 제안하였다.

두 번째로, 우리는 대장균에서 대사 회로를 인지하고, 반응하는 새로운 신호전달 체계를 확인하였다. 대사 회로 의존적 신호전달체계는 하나의 신호만을 인지하는 고전적인 신호전달체계와는 달리 외부의 다양한 신호들이 융합된 복합적 정보를 인식한다는 점에서 효율적인 신호전달체계로 주목받고 있다. 우리는 TCA 회로(tricarboxylic acid cycle)의 마지막 효소인 말산탈수소효소(malate dehydrogenase)가 세포 내 NADH 농도로 대표되는 대사 경로를 인지하고, 단백질 아세틸화효소(lysine acetyltransferase)인 PatZ를 조절한다는 사실을 밝혀내었다. 최종적으로 단백질 아세틸레이션을 통하여, 다양한 생리 및 대사 활성을 조절할 수 있음을 제안하였다.

주요어:

대사신호, 당 수송 인산전달계, c-di-GMP, 대사 회로 의존적 신호전달체계, 단백질아세틸화효소

학번: 2014-21270